# Model reduction in nonlinear dynamics

# Model Reduction in Nonlinear Dynamics

Paul M. A. Slaats

WFW-report 92.106

September 1992

Computational and Experimental Mechanics Group (WFW)
Department of Mechanical Engineering
Eindhoven University of Technology

# Contents

# Abstract

In multibody dynamics, deformations of one or more bodies in the system may be relevant to the dynamical behaviour of the total system, especially when the occurring deformations become large. Aim of research is to find an efficient and general way to describe large deformations in multibody dynamics. In this report, the attention is focussed rather on structural dynamics than on multibody dynamics. Displacements due to deformation are approximated by the modal synthesis method. Since traditional (eigen)modes only occur in linear dynamics and are not defined in nonlinear dynamics, a method to select 'modes' to reduce the system degrees of freedom is proposed, even for the case where deformations become large. Although this method reduces computer processing time, a loss of accuracy in the solution occurs. The error in the approximate solution can be limited by choosing a proper set of modes. A general recipe for this choice is not obvious, e.g. deformation modes highly depend on the boundary conditions of the problem. The basic idea of the method is tested by some numerical bar element examples.

# Nomenclature

| | |
|---|---|
| $\dot{a}$ | time derivative of scalar $a$ |
| $\delta a$ | variation of scalar $a$ |
| $\vec{a}$ | vector |
| $\underset{\sim}{a}$ | column containing scalars |
| $\mathbf{A}$ | second order tensor |
| $\underline{A}$ | matrix containing scalars |
| $\underset{\sim}{a}^T$ | transposed column $\underset{\sim}{a}$ |
| $\mathbf{A^c}$ | conjugate of tensor $\mathbf{A}$ |
| $\underline{A}^{-1}$ | inverse of matrix $\underline{A}$ |
| $\vec{a} \cdot \vec{b}$ | scalar product of vectors $\vec{a}$ and $\vec{b}$ |
| $\mathbf{A} \cdot \vec{a}$ | scalar product of tensor $\mathbf{A}$ and vector $\vec{a}$, resulting in a vector (mapping of $\vec{a}$) |
| $\frac{\partial \underset{\sim}{a}}{(\partial \underset{\sim}{b})^T}$ | jacobian of $\underset{\sim}{a}$ with respect to $\underset{\sim}{b}$ ($\frac{\partial \underset{\sim}{a}}{(\partial \underset{\sim}{b})^T} = \left[\frac{\partial \underset{\sim}{a}}{\partial b_1} \quad \dots \quad \frac{\partial \underset{\sim}{a}}{\partial b_n}\right]$) |

# Chapter 1

# Introduction

## 1.1 General scope of research

Within the field of multibody dynamics, deformations can play a major role in the dynamical behaviour of multibody systems, especially when the occurring deformations become large. The aim of the research project is to find an efficient and general way to describe large deformations in multibody dynamics. In this report, the attention is focussed rather on structural dynamics (i.e. deformations) of one body (or structure) than on the dynamics of a complete multibody system, consisting of several bodies: if large deformations of a body (or structure) are properly described, the idea exists that this description can fit within the framework of the multibody dynamics description without too much effort. The equations of motion of a deformable body are presented in Section 1.2.

Displacements of a deformable body (or structure) are considered to be built up of two kinds of displacements: displacements due to rigid body motion and displacements due to deformations (see Section 1.3). Starting from this kinematic description, two alternative approaches to describe large deformations in multibody dynamics are mentioned: the finite element method and the modal synthesis method. For these two alternatives, attention is focussed on displacements due to deformation, since displacements due to rigid body motion can be superposed later on in the multibody dynamics description.

At first, the finite element method to describe displacements due to deformations is explained in Section 1.4. A finite element discretization can be performed for each body (or structure) as a separated part of the total multibody system. Later on (i.e. in the multibody dynamics description), the nodal degrees of freedom of all deformable parts can be added to the usual rigid body degrees of freedom (3 translations and 3 rotations for each body) of the multibody system. A tough problem encountered when using the finite element approach is the large number of degrees of freedom inherent to the finite element method.

A second approach is based on the so-called "modal synthesis method", known from applications in the field of small deformation multibody dynamics, and now to be tried out in case of large deformations (Section 1.5). In this approach, displacements due to

deformations are approximated by a linear combination of assumed displacement fields. These displacement fields can be obtained by static or dynamic (not necessarily eigenvalue) analyses, preceding the multibody computations. A great advantage of the modal synthesis method as compared to the finite element approach is the small number of degrees of freedom to be considered in the multibody computations. In view of this advantage, the choice for the modal synthesis method seems appropriate. A strategy to select large deformation modes for the modal synthesis method is described in Section 1.6.

Another option to describe large deformations in multibody dynamics is to subdivide a deformable body into several substructures, interconnected by rigid joints. In this way, geometrical nonlinearities are handled by large displacements due to rigid body motion of each substructure, whereas the displacements due to deformation of each substructure remain small. This approach, often referred to as 'substructuring' in literature, has the same disadvantage as the approach where the finite element method is used to describe displacements due to deformations for one body (or structure): the occurrence of a large number of degrees of freedom. Since the approach with the modal synthesis method is expected to involve less degrees of freedom, substructuring is not discussed in this report any further.

## 1.2 The equations of motion of a deformable body

In this section, the equations of motion of a deformable body according to Koppens [1] are reviewed. Expressions for the acceleration vector $\ddot{\vec{r}}$ and the virtual displacement vector $\delta\vec{r}$ are obtained by considering the current configuration as the result of a deformation of the body ($\vec{u}$), a rigid body rotation ($\mathbf{Q}$), and a rigid body translation ($\vec{c}$), consecutively.

$$\ddot{\vec{r}} = \ddot{\vec{c}} + \mathbf{Q} \cdot \left( \vec{\omega} * [\vec{\omega} * (\vec{x} + \vec{u})] + \dot{\vec{\omega}} * (\vec{x} + \vec{u}) + 2\vec{\omega} * \dot{\vec{u}} + \ddot{\vec{u}} \right). \tag{1.1}$$

$$\delta\vec{r} = \delta\vec{c} + \mathbf{Q} \cdot (\delta\vec{\pi} * (\vec{x} + \vec{u}) + \delta\vec{u}). \tag{1.2}$$

where $\vec{\omega}$ and $\delta\vec{\pi}$ are the axial vectors of the skew-symmetric tensors $\mathbf{Q}^c \cdot \dot{\mathbf{Q}}$ and $\mathbf{Q}^c \cdot \delta\mathbf{Q}$, respectively.

Eqs. (1.1) and (1.2) may be substituted in the equations of motion, based on D'Alembert's principle of virtual work,

$$-\delta U + \int_{\Omega_0} \rho_0 \vec{b} \cdot \delta\vec{r} d\Omega_0 - \int_{\Omega_0} \rho_0 \ddot{\vec{r}} \cdot \delta\vec{r} d\Omega_0 + \int_{\Gamma_0} \vec{p} \cdot \delta\vec{r} d\Gamma_0 = 0, \tag{1.3}$$

where

- $\delta U$ is the variation of the strain energy of the body.
- $\Omega_0$ is the reference volume of the body.
- $\rho_0$ is the density of the body in the reference configuration.
- $\vec{b}$ is a specific body load vector.
- $\vec{p}$ is a prescribed surface load per unit of undeformed area.

resulting in

$$
\begin{aligned}
&-\delta U + \int_{\Omega_0} \rho_0 \vec{b} \cdot [\delta\vec{c} + \mathbf{Q} \cdot (\delta\vec{\pi} * (\vec{x} + \vec{u}) + \delta\vec{u})]\, d\Omega_0 \\
&- \int_{\Omega_0} \rho_0 \left[\ddot{\vec{c}} + \mathbf{Q} \cdot \left(\vec{\omega} * [\vec{\omega} * (\vec{x} + \vec{u})] + \dot{\vec{\omega}} * (\vec{x} + \vec{u}) + 2\vec{\omega} * \dot{\vec{u}} + \ddot{\vec{u}}\right)\right] \cdot \\
&\cdot [\delta\vec{c} + \mathbf{Q} \cdot (\delta\vec{\pi} * (\vec{x} + \vec{u}) + \delta\vec{u})]\, d\Omega_0 \\
&+ \int_{\Gamma_0} \vec{p} \cdot [\delta\vec{c} + \mathbf{Q} \cdot (\delta\vec{\pi} * (\vec{x} + \vec{u}) + \delta\vec{u})]\, d\Gamma_0 = 0.
\end{aligned} \tag{1.4}
$$

The second integral in Eq. (1.4) can be elaborated, as has been done by Koppens [1]. The resulting terms are formed by products of $\delta\vec{c}$, $\delta\vec{\pi}$, and $\delta\vec{u}$ on the one hand, and $\ddot{\vec{c}}$, $\mathbf{Q}$, $\vec{\omega}$, $\dot{\vec{\omega}}$, $\vec{u}$, $\dot{\vec{u}}$, $\ddot{\vec{u}}$ on the other hand; and so they turn out to be nonlinear and highly coupled. Yet, by resolving displacements into displacements due to rigid body motion and displacements due to deformation, a "Ritz-kind-of" method can be used to reduce the number of degrees of freedom.

So far, the expression for the variation of the strain energy has not been discussed. Of course, the strain energy of a body depends on the displacements due to deformation. Koppens [1] mentions that expressions for the variation of the strain energy are too complicated to evaluate, in general. For example, linearized strain measures are often used in the expression. Also the body may be approximated by (e.g) a one dimensional body in case two dimensions of the body are considerably smaller than the other dimension using an assumption from which the displacements of an arbitrary material point of the body can be written in terms of the displacement of a line. With such a one-dimensional body goes an approximate expression for its strain energy. A beam is an example of such a body. An example of an expression for the strain energy is provided below (from [2])

$$
\begin{aligned}
U &= \frac{E}{2} \int_{\Omega} \epsilon_{xx}^2 d\Omega \\
&= \frac{EA}{2} \int_0^l \left(\frac{\partial u}{\partial x}\right)^2 dx + \frac{EI}{2} \int_0^l \left(\frac{\partial^2 v}{\partial x^2}\right)^2 dx.
\end{aligned} \tag{1.5}
$$

where $E$ is the Young's modulus, $\Omega$ is the beam volume, $A$ is the beam cross section area, $\epsilon_{xx}$ is the axial strain measure, $l$ is the beam length, $u$ is the longitudinal displacement, $v$ is the transversal displacement, $x$ is the coordinate along the longitudinal beam axis, and $I$ is the area moment of inertia of the beam. In case nonlinear contributions of the strain are taken into consideration, the strain energy has another (more extensive) form:

$$
U_{nl} = \frac{EA}{2} \int_0^l \left(\frac{\partial u}{\partial x}\right)^2 dx + \frac{EI}{2} \int_0^l \left(\frac{\partial^2 v}{\partial x^2}\right)^2 dx + \frac{EA}{2} \int_0^l \frac{\partial u}{\partial x} \left(\frac{\partial v}{\partial x}\right)^2 dx. \tag{1.6}
$$

## 1.3 Rigid body motions and deformations

The displacement of a deformable body in a multibody system can be resolved into displacement due to a rigid body motion and displacement due to deformation. Large displacements

are quite common in multibody dynamics, since the joints occurring in a multibody system enable the bodies to go through large translations and large rotations with respect to each other. Examples of such joints are revolute, cylindrical, spherical, and translational joints.

If also large deformations of a body are considered, the displacements due to deformation become large. This means that an elementary line element between two material points in the reference configuration can experience a large elongation and a moderately large rotation in the deformed configuration. Rotations due to deformation can be "finite", but not unrestricted as in the case of rigid body rotations. Displacements due to large deformations can be described with respect to a reference frame that moves with respect to the inertial frame. In case the reference frame moves in correspondance to the rigid body motion of the largely deformable body, then a separation between displacements as a rigid body and displacements due to deformation is reached.

A reference frame that moves with the body in space is also called a "body-fixed reference frame" or a "co-rotational reference frame". Vu-Quoc [3] and Simo & Vu-Quoc [4] call it a "floating frame", and they discuss such an approach for a flexible beam. In this approach, they mention a so-called "shadow beam approach: a classical approach based on small strains superposed on large rigid body rotations". Vu-Quoc's thesis [3] shows that by using this approach the equations of motion are nonlinear and highly coupled in the inertia terms. The resulting equations of motion by using this approach are given by Eq. (1.4).

Vu-Quoc [3] and Simo & Vu-Quoc [4] propose an alternative approach, in which motion is represented with respect to an inertial reference frame. In this way, the expression for the kinetic energy is simply reduced to a quadratic uncoupled form. Determination of the potential energy starts from the expression for the potential energy in the case of the small strain shadow beam approach, and in this expression, strain components with respect to the inertial frame are substituted (see [3], p.19). Essential in Vu-Quoc's approach is the use of structural theories (rods, plates, shells, 3D continua, etc.) whose appropriate strain measures possess the required property of objectivity (i.e. invariance with respect to rigid body motions). However, Vu-Quoc's approach does not tend to reduce the number of degrees of freedom, since large rigid body rotations with respect to inertial reference frame can not be included in the modal synthesis method. Since the aim of our research is to describe large deformations with the smallest possible number of degrees of freedom in order to reduce computation times, Vu-Quoc's approach is not further discussed.

Resuming, we consider displacements of a deformable body (or structure) to be built up of two kinds of displacements: displacements due to rigid body motion and displacements due to deformations. Starting from this kinematic description, two alternative approaches to describe large deformations in multibody dynamics are briefly discussed in the next two sections. For these two alternatives, attention is focussed on displacements due to deformation.

## 1.4 First approach: the finite element method integrated with the multibody analysis

The deformations of a flexible body, in Section 1.2 denoted by a vector field $\vec{u}$, can be approximated by a finite element approach. In this case, a mesh with (often many) nodes is generated, where every node has several degrees of freedom. The number of degrees of freedom per node depends on the type of elements used. Displacements of material points in between the nodes can be computed by interpolation of the nodal displacements. Therefore, interpolation functions are defined. One interpolation function is assigned to each nodal degree of freedom: the value of this interpolation function equals one in that specific node, and equals zero in all the other nodes; the only other part of the domain where that specific interpolation function is unequal to zero is formed by the elements that the node belongs to. The interpolation functions of all nodes can be organized (or assembled) in a matrix column as follows:

$$\underset{\sim}{\vec{\phi}}^{int} = \begin{bmatrix} \vec{\phi}_1^{int} \\ \vec{\phi}_2^{int} \\ \cdot \\ \cdot \\ \cdot \\ \vec{\phi}_n^{int} \end{bmatrix} \tag{1.7}$$

where $n$ equals the number of nodal degrees of freedom, and where all elements of the column $\underset{\sim}{\vec{\phi}}^{int}$ depend on the position ($\vec{x}_0$) in the reference configuration:

$$\underset{\sim}{\vec{\phi}}^{int} = \underset{\sim}{\vec{\phi}}^{int}(\vec{x}_0) \tag{1.8}$$

With this definition, the displacement vector $\vec{u} = \vec{u}(\vec{x}_0, t)$ can be denoted as

$$\vec{u}(\vec{x}_0, t) = \underset{\sim}{\alpha}(t)^T \underset{\sim}{\vec{\phi}}^{int}(\vec{x}_0) \tag{1.9}$$

From a physical standpoint, the elements of $\underset{\sim}{\alpha}$ correspond to nodal degrees of freedom (also called nodal coordinates). They are a function of time and gathered in column $\underset{\sim}{\alpha}(t)$. If Eq. (1.9) is substituted in the equation of motion (Eq. (1.4)) and if all these time-dependent nodal degrees of freedom are taken into consideration, time integration of the equation of motion becomes impractical, especially in case of a complex geometry with many nodes and many degrees of freedom.

## 1.5 Second approach: the modal synthesis method

The finite element method leads to models with many degrees of freedom, and integration of the total system of differential equations with these many degrees of freedom results in large computation times. Koppens [1] mentions that many degrees of freedom lead to

a large range of eigenfrequencies which reduces the integration time steps and increases computation time. This forms another reason to aim at a reduction of degrees of freedom. A practicable way to achieve this is by using the modal synthesis method.

A mode (or mode shape) is a possible displacement pattern of the nodes of a flexible body [5]. Suppose that $m$ modes are gathered in the columns of a matrix $\underline{\Phi}$. Each mode is a column with displacements at a discrete number of points (i.e. the nodes), and interpolation between these discrete values results in "continuous modes". The discrete modes can be multiplied by the same interpolation functions as mentioned in the previous section:

$$\underset{\sim}{\vec{\phi}} = \underline{\Phi}^T \underset{\sim}{\vec{\phi}}^{int} \tag{1.10}$$

where $\underline{\Phi}$ is an $n$ x $m$ matrix of constant nodal displacements.

By this transformation, a reduced set of base functions is obtained, since $m$ will be much smaller than $n$ in general. In fact, the dimension of $m$ depends on the type of the problem, and is determined by the engineer.

Again, like in the previous section, the displacement vector $\vec{u} = \vec{u}(\vec{x}_0, t)$ can be denoted as the product of two functions: a function of time and a function of positions in the reference configuration

$$\vec{u}(\vec{x}_0, t) = \underset{\sim}{\vec{\phi}}(\vec{x}_0)^T \underset{\sim}{\alpha}(t) \tag{1.11}$$

In this way, $\underset{\sim}{\alpha}(t)$ may be considered as a column with (kind of like) amplification factors. In the integration process of the multibody system, the values of the elements in $\underset{\sim}{\alpha}(t)$ will show which modes are important in a flexible analysis, and which modes are irrelevant.

Two types of modes can be used in the modal synthesis method: static and dynamic modes.

Static modes can be obtained by solving the static equilibrium equation

$$\underline{K}\,\underset{\sim}{u} = \underset{\sim}{F} \tag{1.12}$$

where $\underline{K}$ is the stiffness matrix with respect to the nodal degrees of freedom, $\underset{\sim}{u}$ is a column with nodal displacements, and $\underset{\sim}{F}$ is an applied static force. In case of geometrically non-linear deformations, the stiffness matrix $\underline{K}$ is not constant anymore, and it depends on the deformed configuration of the system. An incremental approach is needed then, in which a (e.g.) Newton-Raphson procedure may converge to solutions per increment.

Usually in linear dynamics, modes are obtained by solving an eigenvalue problem

$$\underline{M}\,\ddot{\underset{\sim}{u}} + \underline{K}\,\underset{\sim}{u} = \underset{\sim}{0}, \tag{1.13}$$

where $\underline{M}$ represents the (either lumped or consistent) mass matrix with respect to the finite element degrees of freedom. By prescribing suitable boundary conditions, rigid body motion can be suppressed. If the boundary conditions still allow rigid body motions, then eigenvalues equal to zero will occur in the eigenvalue problem. By eliminating the eigenfunctions corresponding to the zero eigenfrequencies, rigid body motion is also avoided in the modal synthesis method. The eigenvalue problem is only applicable to linear systems though. For nonlinear dynamics (without damping), the equations of motion for a body (represented by $n$ finite element nodes) can be denoted as

$$\underline{M}\ddot{\underset{\sim}{u}} = \underset{\sim}{f}_e(t) - \underset{\sim}{f}_i(\underset{\sim}{u}) \tag{1.14}$$

in which $\underset{\sim}{f}_i$ contains internal nodal forces, nonlinear in displacements, and $\underset{\sim}{f}_e$ contains prescribed external nodal forces, known as a function of time. Matrix $\underline{M}$ can be either lumped or consistent (e.g. see next chapter).

A possible way to determine dynamic modes for the nonlinear case will be presented in Chapter 3

## 1.6 Computational strategy

As already mentioned in Section 1.1, the choice for the modal synthesis method seems appropriate because of the small number of degrees of freedom to be considered in the multibody computations.

A problem yet to overcome when using the modal synthesis method for large deformations is the selection of a proper set of deformation modes to reduce the number of system degrees of freedom. Two strategies have been devised to face this problem.

The first strategy is based on the selection of 'arbitrary modes in time' and/or nonlinear static modes. The term 'arbitrary modes in time' refers to deformation modes that satisfy certain user defined criteria, e.g. modes corresponding to potential or kinetic energy maxima obtained by transient analyses of the system, possibly with slightly different boundary conditions. These arbitrary modes in time will also be named 'alternative modes' or 'dynamic modes' in this report, having no correspondence whatsoever with modes obtained from an eigenvalue problem (such as modes used in the component mode synthesis). Static modes are obtained by solving the set of nonlinear algebraic equations that results after neglecting inertia terms in the original ordinary differential equations (ODE) of the system.

The second strategy is based on the selection of so-called 'tangent modes' and 'modal derivatives', obtained from the linearized system, and can also be spotted in some earlier literature articles (Refs. [6], [7], [8], [9]). Tangent modes and modal derivatives depend on the time instant of linearization. At a certain instant of time, the originally nonlinear second order ODE's are linearized, and a (tangent) stiffness matrix and mass matrix enable the eigenvalue problem to be solved for (tangent- or) eigenmodes, from which the modal derivatives can be derived later on.

Both strategies can be implemented in such a way that the set of deformation modes is updated when the approximate solution obtained by the modal synthesis method does not satisfy the original system equations well enough. Updating the set of deformation modes in time will not be considered in this report though: we restrict ourselves to a constant set of deformation modes.

This report is limited to a description of the first strategy. In illustration of the second strategy, the reader is referred to Ref. [10]. The basic ideas are illustrated by analyses of bar element systems.

# Chapter 2

# Large Deformation Dynamic Analysis of Bar Structures

## 2.1 Introduction

In this report, attempts to try out the idea of reducing nonlinear dynamical models are practiced for bar element structures. In Section 2.2, the dynamics of a bar element are presented. Displacements of the element nodes due to deformation represent the element degrees of freedom. Elements are interconnected according to a certain topology array, and with this array the usual assembly process for the complete bar element structure can be carried out. When the assembled nonlinear dynamic system is integrated in time, slight integration errors occur, and depending on the type of integration method, these errors remain limited or increase in time. Integration errors are evaluated in Section 2.3 by defining energy (and also power) residues of the system equations of motion.

## 2.2 Dynamics of a bar element

Very generally, we start from the equations representing local balance of linear momentum at an interior point of the element referring to the reference configuration (Koppens, 1989 [1])

$$\vec{\nabla}_0 \cdot (\mathbf{P}_2 \cdot \mathbf{F}^c) + \rho_0 \vec{f} = \rho_0 \ddot{\vec{u}} \qquad \forall \vec{u} \tag{2.1}$$

in which

| | |
|---|---|
| $\vec{\nabla}_0$ | gradient with respect to the reference configuration |
| $\mathbf{P_2}$ | second Piola-Kirchhoff stress tensor |
| $\mathbf{F}$ | deformation tensor |
| $\rho_0$ | density in reference configuration |
| $\vec{f}$ | external load per unit of mass |
| $\vec{u}$ | displacement (due to deformation) |
| $\ddot{\vec{u}}$ | acceleration |

and according to D'Alembert's principle of virtual work

$$\int_{\Omega_0} \left(\vec{\nabla}_0 \cdot (\mathbf{P_2} \cdot \mathbf{F}^c) + \rho_0(\vec{f} - \ddot{\vec{u}})\right) \cdot \delta\vec{u} d\Omega_0 = 0 \qquad \forall \delta\vec{u} \tag{2.2}$$

($\Omega_0$ is the element volume in the reference configuration) the weak formulation follows by partial integration

$$\int_{\Gamma_0} \vec{p} \cdot \delta\vec{u} d\Gamma_0 + \int_{\Omega_0} \rho_0(\vec{f} - \ddot{\vec{u}}) \cdot \delta\vec{u} d\Omega_0 - \int_{\Omega_0} (\vec{\nabla}_0 \delta\vec{u})^c : (\mathbf{P_2} \cdot \mathbf{F}^c) d\Omega_0 = 0 \ \ \forall \delta\vec{u} \tag{2.3}$$

($\Gamma_0$ is the element boundary in the reference configuration) where $\vec{p}$ is the surface load per unit of undeformed area

$$\vec{p} = \vec{n}_0 \cdot \mathbf{P_2} \cdot \mathbf{F}^c = \mathbf{F} \cdot \mathbf{P_2} \cdot \vec{n}_0 \tag{2.4}$$

The equations can be specified for the bar element as illustrated in Fig. 2.1.

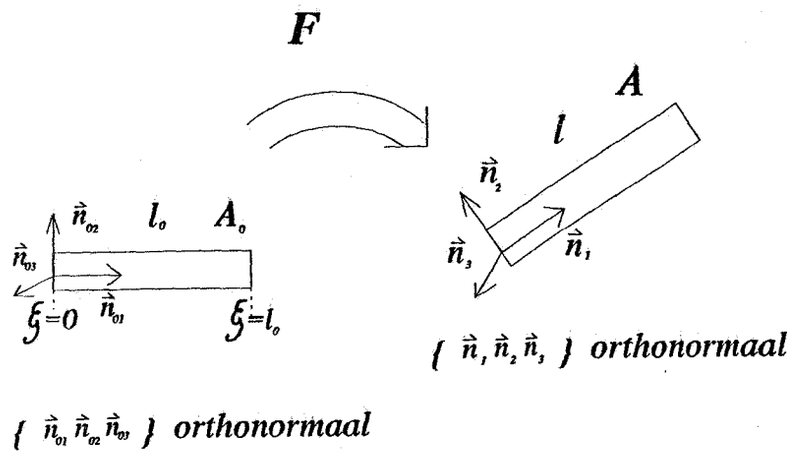


Figure 2.1: *3D bar element in reference and present configuration*

$$\delta\vec{u} = (1 - \frac{\xi}{l_0})\delta\vec{u}_1 + \frac{\xi}{l_0}\delta\vec{u}_2 \tag{2.5}$$

with $\delta\vec{u}_1 = \delta\vec{u}(\xi = 0)$ and $\delta\vec{u}_2 = \delta\vec{u}(\xi = l_0)$.
The first term in Eq. (2.3) is worked out as

$$\int_{\Gamma_0} \vec{p} \cdot \delta\vec{u} d\Gamma_0 = \vec{p}_1 \cdot \delta\vec{u}_1 + \vec{p}_2 \cdot \delta\vec{u}_2 \tag{2.6}$$

The second term of Eq. (2.3) can be worked out according to either a "lumped-mass approach" or a "consistent-mass approach".

- In the lumped-mass approach, the mass of the element is equally lumped to the two element nodes (it is assumed that the mass of the element is uniformly distributed over the element)

$$\int_{\Omega_0} \rho_0(\vec{f} - \ddot{\vec{u}}) \cdot \delta\vec{u} d\Omega_0 \approx \frac{1}{2} m(\delta\vec{u}_1 \cdot (\vec{f} - \ddot{\vec{u}}_1) + \delta\vec{u}_2 \cdot (\vec{f} - \ddot{\vec{u}}_2)) \tag{2.7}$$

  where $m = \rho_0 A_0 l_0$ represents the total mass of the bar.

- In the consistent-mass approach, the integral is neatly worked out (see Eq. (2.5) for $\delta\vec{u}(\xi)$, the same interpolation goes for $\ddot{\vec{u}}(\xi)$)

$$\int_{\Omega_0} \rho_0(\vec{f} - \ddot{\vec{u}}) \cdot \delta\vec{u} d\Omega_0 = \rho_0 A_0 \int_{\xi=0}^{l_0} \vec{f} \cdot \delta\vec{u}(\xi) d\xi - \rho_0 A_0 \int_{\xi=0}^{l_0} \ddot{\vec{u}}(\xi) \cdot \delta\vec{u}(\xi) d\xi \tag{2.8}$$

  and after some elaborations

$$\int_{\Omega_0} \rho_0(\vec{f} - \ddot{\vec{u}}) \cdot \delta\vec{u} d\Omega_0 = m(\delta\vec{u}_1 \cdot (\frac{1}{2}\vec{f} - (\frac{1}{3}\ddot{\vec{u}}_1 + \frac{1}{6}\ddot{\vec{u}}_2)) + \delta\vec{u}_2 \cdot (\frac{1}{2}\vec{f} - (\frac{1}{6}\ddot{\vec{u}}_1 + \frac{1}{3}\ddot{\vec{u}}_2))) \tag{2.9}$$

Finally, for elaborating the third term in Eq. (2.3), we write the second Piola-Kirchhoff tensor and the Cauchy stress tensor as (according to Schreurs [11])

$$\mathbf{P_2} = s\vec{n}_{01}\vec{n}_{01} \tag{2.10}$$

$$\sigma = \sigma\vec{n}_1\vec{n}_1 \tag{2.11}$$

($s$: axial $2^{nd}$ Piola-Kirchhoff stress component; $\sigma$: axial component of the Cauchy stress tensor $\boldsymbol{\sigma}$)

$$\mathbf{U} = \lambda\vec{n}_{01}\vec{n}_{01} + \mu(\vec{n}_{02}\vec{n}_{02} + \vec{n}_{03}\vec{n}_{03}) \tag{2.12}$$

in which

| | |
|---|---|
| $\mathbf{U}$ | elongation tensor |
| $\lambda$ | elongation ratio ($\lambda = \frac{l}{l_0}$) |
| $\mu$ | contraction ratio ($\mu = \sqrt{\frac{A}{A_0}}$) |

$$\mathbf{R} = \vec{n}_1\vec{n}_{01} + \vec{n}_2\vec{n}_{02} + \vec{n}_3\vec{n}_{03} \tag{2.13}$$

where $\mathbf{R}$ is the rotation tensor.

$$\begin{aligned} \mathbf{F} &= \mathbf{R}\cdot\mathbf{U} = \\ &= \lambda\vec{n}_1\vec{n}_{01} + \mu(\vec{n}_2\vec{n}_{02} + \vec{n}_3\vec{n}_{03}) \end{aligned} \tag{2.14}$$

$$\vec{\nabla}_0 = \vec{n}_{01}\frac{d}{d\xi} \tag{2.15}$$

By combining Eqs. (2.5), (2.10), (2.14) and (2.15), the third term in Eq. (2.3) can be worked out

$$\begin{aligned} \int_{\Omega_0}(\vec{\nabla}_0\delta\vec{u})^c : (\mathbf{P}_2\cdot\mathbf{F}^c)d\Omega_0 &= A_0\int_{\xi=0}^{l_0}(\vec{n}_{01}\frac{1}{l_0}(-\delta\vec{u}_1 + \delta\vec{u}_2))^c : (s\lambda\vec{n}_{01}\vec{n}_1)d\xi \\ &= \frac{A_0}{l_0}\int_{\xi=0}^{l_0}(-\delta\vec{u}_1 + \delta\vec{u}_2)\cdot s\lambda\vec{n}_1 d\xi \end{aligned} \tag{2.16}$$

The relation between $\mathbf{P}_2$ and $\sigma$ is

$$\begin{aligned} \sigma &= J^{-1}\mathbf{F}\cdot\mathbf{P}_2\cdot\mathbf{F}^c \\ &= \frac{s}{J}\lambda^2\vec{n}_1\vec{n}_1 \\ &= \sigma\vec{n}_1\vec{n}_1 \end{aligned} \tag{2.17}$$

where $J = det(\mathbf{F})$, and so

$$s = \frac{J\sigma}{\lambda^2} \tag{2.18}$$

Several constitutive relationships can be chosen now, e.g.:

- a linear relation between the axial Cauchy stress component and the axial strain component $\varepsilon$

  $$\sigma = E\varepsilon \tag{2.19}$$

  where $E$ is the Young's modulus, and $\varepsilon$ is defined in terms of a chosen (possibly nonlinear) strain-displacement relation, e.g.:

  - linear strain (i.e. linear in $\lambda$!)

    $$\varepsilon = \lambda - 1 \tag{2.20}$$

  - Green-Lagrange strain (nonlinear)

    $$\varepsilon = \frac{1}{2}(\lambda^2 - 1) \tag{2.21}$$

  - logarithmic strain (nonlinear)

$$\varepsilon = \ln(\lambda) \tag{2.22}$$

- the axial Cauchy stress component expressed as a nonlinear function of the elongation ratio at first hand, e.g.:
  - Neo-Hookean material model

$$\sigma = c_1(\lambda^2 - \frac{1}{\lambda}) \tag{2.23}$$

  - Mooney-Rivlin material model

$$\sigma = c_1(\lambda^2 - \frac{1}{\lambda}) + c_2(\lambda - \frac{1}{\lambda^2}) \tag{2.24}$$

  where $c_1$ in Eqs. (2.23) and (2.24) and $c_2$ in Eq. (2.24) are material constants. Fig. 2.2 shows two curves corresponding to the material models of Eqs. (2.23) and (2.24) (first Piola-Kirchhoff axial stress equals $\frac{\sigma}{\lambda}$).

For the ease of further derivations, we consider the material to be incompressible

$$\begin{aligned} J &= det(\mathbf{F}) \\ &= 1 \end{aligned} \tag{2.25}$$

which definitely is the case for Neo-Hookean and Mooney-Rivlin models, but is an extra assumption for the models according to Eqs. (2.20), (2.21), and (2.22).
With Eqs. (2.18) and (2.25), Eq. (2.16) becomes

$$\frac{A_0}{l_0}\int_{\xi=0}^{l_0}(-\delta\vec{u}_1 + \delta\vec{u}_2)\cdot\frac{\sigma}{\lambda}\vec{n}_1 d\xi = (-\delta\vec{u}_1 + \delta\vec{u}_2)\cdot\frac{A_0\sigma}{\lambda}\vec{n}_1 \tag{2.26}$$

Back to Eq. (2.3); by combining Eqs. (2.6), (2.26), and (2.7) in case of a lumped-mass approach, (or (2.9) in case of a consistent-mass approach), Eq. (2.3) can be written as

$$\begin{aligned} & \delta\vec{u}_1 \cdot \left\{\vec{p}_1 + \frac{1}{2}m(\vec{f} - \ddot{\vec{u}}_1) + A_0\frac{\sigma}{\lambda}\vec{n}_1\right\} \\ + \quad & \delta\vec{u}_2 \cdot \left\{\vec{p}_2 + \frac{1}{2}m(\vec{f} - \ddot{\vec{u}}_2) - A_0\frac{\sigma}{\lambda}\vec{n}_1\right\} = 0 \quad \forall\delta\vec{u}_1, \delta\vec{u}_2 \end{aligned} \tag{2.27}$$

After discussing the general three dimensional case, we now restrict ourselves to two dimensions. Representation in the $\{\vec{e}_1, \vec{e}_2\}$-plane (see Fig. 2.3):

$$l = \sqrt{(y_j - y_i)^2 + (x_j - x_i)^2} \tag{2.28}$$

$$l_0 = \sqrt{(y_{j0} - y_{i0})^2 + (x_{j0} - x_{i0})^2} \tag{2.29}$$

$$\vec{n}_1 = \frac{x_j - x_i}{l}\vec{e}_1 + \frac{y_j - y_i}{l}\vec{e}_2 \tag{2.30}$$

with

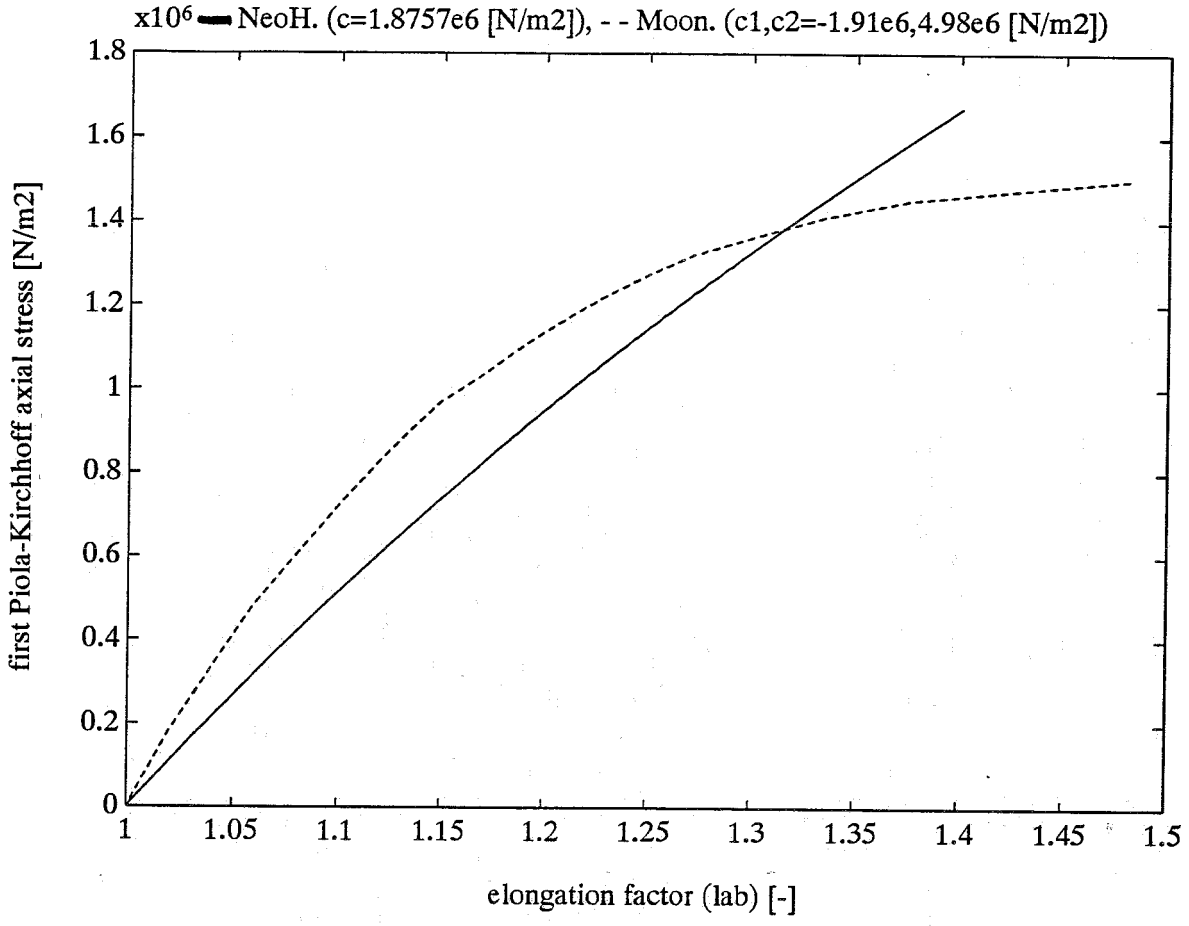


Figure 2.2: *Neo-Hookean and Mooney-Rivlin material models*

$$x_i = x_{0i} + u_i \tag{2.31}$$

$$y_i = y_{0i} + v_i \tag{2.32}$$

$$x_j = x_{0j} + u_j \tag{2.33}$$

$$y_j = y_{0j} + v_j \tag{2.34}$$

If the number of nodes in the complete bar element structure equals $nd$, the total number of degrees of freedom in the system equals $2 * nd$. In case of reduction of the degrees of freedom by using modes and modal coordinates (say: approximation by $m$ modes, then $m < 2 * nd$), then the positions can be expressed in the modal coordinates as follows

$$x_i = x_{0i} + \sum_{k=1}^{m} \phi_{xik}\alpha_k \tag{2.35}$$

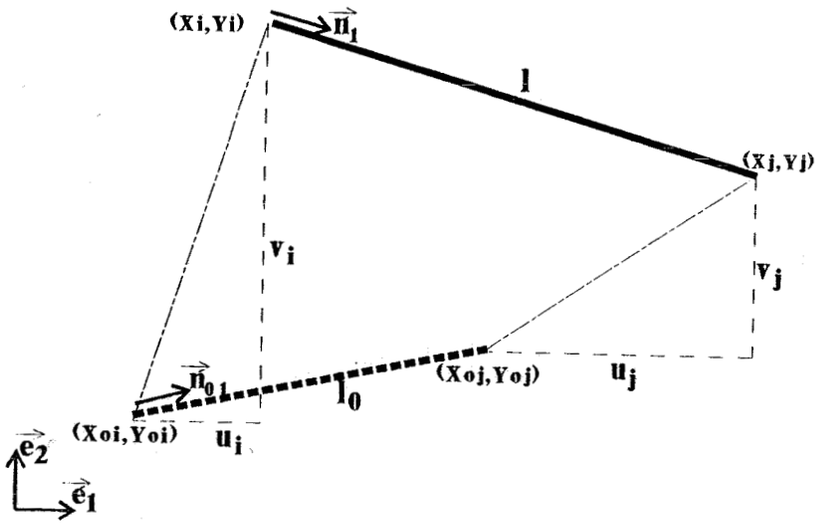


Figure 2.3: *nodal coordinates in the* $\{\vec{e}_1, \vec{e}_2\}$*-plane*

$$y_i = y_{0i} + \sum_{k=1}^{m} \phi_{yik}\alpha_k \tag{2.36}$$

$$x_j = x_{0j} + \sum_{k=1}^{m} \phi_{xjk}\alpha_k \tag{2.37}$$

$$y_j = y_{0j} + \sum_{k=1}^{m} \phi_{yjk}\alpha_k \tag{2.38}$$

And thus, the equations of motion can be built up in terms of nodal degrees of freedom gathered in $\underset{\sim}{u}$ (original system degrees of freedom) or modal coordinates gathered in $\underset{\sim}{\alpha}$ (reduced system degrees of freedom). The following relation between these two columns holds

$$\underset{\sim}{u} = \underline{\Phi}\,\underset{\sim}{\alpha} \tag{2.39}$$

(Column-)matrix representation (with respect to the inertial frame) for implementation results in

$$\begin{aligned} &\left[\begin{array}{cc} \delta\underset{\sim}{u}_1^T & \delta\underset{\sim}{u}_2^T \end{array}\right] \left\{ \left[\begin{array}{c} \underset{\sim}{p}_1 \\ \underset{\sim}{p}_2 \end{array}\right] + \underline{M} \left[\begin{array}{c} \underset{\sim}{f} - \ddot{\underset{\sim}{u}}_1 \\ \underset{\sim}{f} - \ddot{\underset{\sim}{u}}_2 \end{array}\right] - A_0 \frac{\sigma}{\lambda} \left[\begin{array}{c} -\underset{\sim}{n}_1 \\ \underset{\sim}{n}_1 \end{array}\right] \right\} = \\ &= 0 \qquad\qquad \forall \delta\underset{\sim}{u}_1, \delta\underset{\sim}{u}_2 \end{aligned} \tag{2.40}$$

where for the lumped-mass approach

$$\underline{M} = \underline{M}_{lumped} = \begin{bmatrix} \frac{1}{2}m & 0 & 0 & 0 \\ 0 & \frac{1}{2}m & 0 & 0 \\ 0 & 0 & \frac{1}{2}m & 0 \\ 0 & 0 & 0 & \frac{1}{2}m \end{bmatrix} \tag{2.41}$$

or for the consistent-mass approach

$$\underline{M} = \underline{M}_{consistent} = \frac{1}{2}m \begin{bmatrix} \frac{2}{3} & 0 & \frac{1}{3} & 0 \\ 0 & \frac{2}{3} & 0 & \frac{1}{3} \\ \frac{1}{3} & 0 & \frac{2}{3} & 0 \\ 0 & \frac{1}{3} & 0 & \frac{2}{3} \end{bmatrix} \tag{2.42}$$

Eq. (2.40) has been derived for arbitrary $\delta\underset{\sim}{u}_1$ and $\delta\underset{\sim}{u}_2$, and so the following equation must hold

$$\begin{bmatrix} \ddot{\underset{\sim}{u}}_1 \\ \ddot{\underset{\sim}{u}}_2 \end{bmatrix} = \underline{M}^{-1} \begin{bmatrix} \underset{\sim}{p}_1 \\ \underset{\sim}{p}_2 \end{bmatrix} + \begin{bmatrix} \underset{\sim}{f} \\ \underset{\sim}{f} \end{bmatrix} - \underline{M}^{-1} A_0 \frac{\sigma}{\lambda} \begin{bmatrix} -\underset{\sim}{n}_1 \\ \underset{\sim}{n}_1 \end{bmatrix} \tag{2.43}$$

Or abbreviated

$$\ddot{\underset{\sim}{u}} = \underline{M}^{-1}(\underset{\sim}{f}_e - \underset{\sim}{f}_i) \tag{2.44}$$

with nodal accelerations

$$\ddot{\underset{\sim}{u}} = \begin{bmatrix} \ddot{\underset{\sim}{u}}_1 \\ \ddot{\underset{\sim}{u}}_2 \end{bmatrix} \tag{2.45}$$

external forces

$$\underset{\sim}{f}_e = \begin{bmatrix} \underset{\sim}{p}_1 \\ \underset{\sim}{p}_2 \end{bmatrix} + \underline{M} \begin{bmatrix} \underset{\sim}{f} \\ \underset{\sim}{f} \end{bmatrix} \tag{2.46}$$

and internal forces

$$\underset{\sim}{f}_i = A_0 \frac{\sigma}{\lambda} \begin{bmatrix} -\underset{\sim}{n}_1 \\ \underset{\sim}{n}_1 \end{bmatrix} \tag{2.47}$$

When the equations of motion (Eq. (2.40)) are formulated in terms of modal coordinates,

$$\delta\underset{\sim}{\alpha}^T \underline{\Phi}^T \left\{ \underset{\sim}{f}_e - \underline{M}\underline{\Phi}\ddot{\underset{\sim}{\alpha}} - \underset{\sim}{f}_i \right\} = 0 \qquad \forall \delta\underset{\sim}{\alpha} \tag{2.48}$$

then again, we can abbreviate

$$\ddot{\underset{\sim}{\alpha}} = (\underline{M}^r)^{-1}(\underset{\sim}{f}_e - \underset{\sim}{f}_i), \tag{2.49}$$

with the reduced mass matrix,

$$\underline{M}^r = \underline{\Phi}^T \underline{M} \underline{\Phi}, \tag{2.50}$$

reduced external forces,

$$\underset{\sim}{f}_e^r = \underline{\Phi}^T \underset{\sim}{f}_e, \tag{2.51}$$

and reduced internal forces,

$$\underset{\sim}{f}_i^r = \underline{\Phi}^T \underset{\sim}{f}_i. \tag{2.52}$$

For simplification purposes, we restrict ourselves to the following cases:

- no external loads per unit of mass: $\underset{\sim}{f} = \underset{\sim}{0}$
- the surface load per unit of undeformed area is only a function of time: $\underset{\sim}{p} = \underset{\sim}{p}(t)$

With these restrictions, the internal and external forces are functions of displacements and time, respectively:

$$\underset{\sim}{f}_i = \underset{\sim}{f}_i(\underset{\sim}{u}) \tag{2.53}$$

$$\underset{\sim}{f}_e = \underset{\sim}{f}_e(t) \tag{2.54}$$

Transformation to a $1^{st}$ order system for integration purposes (e.g. general Runge Kutta integration methods) results in

$$\begin{bmatrix} \dot{\underset{\sim}{u}} \\ \dot{\underset{\sim}{v}} \end{bmatrix} = \begin{bmatrix} \underset{\sim}{v} \\ \underline{M}^{-1}(\underset{\sim}{f}_e(t) - \underset{\sim}{f}_i(\underset{\sim}{u})) \end{bmatrix} \tag{2.55}$$

or in terms of $\underset{\sim}{\alpha}$:

$$\begin{bmatrix} \dot{\underset{\sim}{\alpha}} \\ \dot{\underset{\sim}{\beta}} \end{bmatrix} = \begin{bmatrix} \underset{\sim}{\beta} \\ (\underline{M}^r)^{-1}(\underset{\sim}{f}_e^r(t) - \underset{\sim}{f}_i^r(\underset{\sim}{\alpha})) \end{bmatrix} \tag{2.56}$$

The column with positions, $\underset{\sim}{x}^T = [x_1 y_1 \ldots x_{nd} y_{nd}]$ with $nd$ denoting the number of nodes, is obtained easily afterwards:

$$\begin{aligned} \underset{\sim}{x} &= \underset{\sim}{x_0} + \underset{\sim}{u} \\ &= \underset{\sim}{x_0} + \underline{\Phi}\underset{\sim}{\alpha}. \end{aligned} \tag{2.57}$$

A final remark must be made about the normalization of the modes in $\underline{\Phi}$. In order to avoid large differences in magnitudes of the modal coordinates, the modes are 'normalized with respect to the mass matrix $\underline{M}$'. Since 'arbitrary modes in time' and static modes are not orthogonal with respect to $\underline{M}$ (as is the case for eigenmodes in linear dynamics), the reduced mass matrix $\underline{M}^r$ in Eq. (2.50) will not be a diagonal matrix. Yet, if we want to scale the modes, we can just consider the diagonal elements of $\underline{M}^r$ and make these elements equal to one, by reassigning the modes

$$\underset{\sim}{\phi}_i := \frac{\underset{\sim}{\phi}_i}{\sqrt{\underset{\sim}{\phi}_i^T \underline{M} \underset{\sim}{\phi}_i}}. \tag{2.58}$$

## 2.3 Energy, power, and integration residues

Three types of energy can be distinguished in the system equations of motion:

- externally applied work by the external forces (from $\tau = 0$ to $\tau = t$)

$$W = \underset{\sim}{f}_e \cdot \underset{\sim}{u} \tag{2.59}$$

- kinetic energy of the nodal masses

$$T = \sum_{i=1}^{nd} \frac{1}{2} m_i \dot{\underset{\sim}{u}}_i^T \dot{\underset{\sim}{u}}_i \tag{2.60}$$

where $nd$ denotes the total number of nodes in the system, and $m_i$ represents the mass of node $i$ here.

- potential energy; since gravity is not taken into account, only elastic energy in the bars results in potential energy. In Eq. (2.40), we can recognize the variation of the strain energy for one bar element

$$\delta U = A_0 \frac{\sigma}{\lambda} \delta l \tag{2.61}$$

where

$$\delta l = \begin{bmatrix} \delta \underset{\sim}{u}_1^T & \delta \underset{\sim}{u}_2^T \end{bmatrix} \cdot \begin{bmatrix} -\underset{\sim}{n}_1 \\ \underset{\sim}{n}_1 \end{bmatrix} \tag{2.62}$$

Depending on the chosen constitutive relation, the potential energy can be derived, e.g.

  - by using Eq. (2.20)

$$U = EA_0 l_0 \left(\frac{l}{l_0} - 1 - \ln\left(\frac{l}{l_0}\right)\right) \tag{2.63}$$

  - or by Eq. (2.21)

$$U = \frac{1}{2} EA_0 l_0 \left(\frac{1}{2}\left(\frac{l}{l_0}\right)^2 - \ln\left(\frac{l}{l_0}\right) - \frac{1}{2}\right) \tag{2.64}$$

  - or by Eq. (2.22)

$$U = \frac{1}{2} EA_0 l_0 \left(\ln\left(\frac{l}{l_0}\right)\right)^2 \tag{2.65}$$

  - or by Eq. (2.23)

$$U = c_1 A_0 l_0 (\frac{1}{2}(\frac{l}{l_0})^2 + \frac{l_0}{l} - \frac{3}{2}) \tag{2.66}$$

– or by Eq. (2.24)

$$U = c_1 A_0 l_0 (\frac{1}{2}(\frac{l}{l_0})^2 + \frac{l_0}{l} - \frac{3}{2}) + c_2 A_0 l_0 (\ln(\frac{l}{l_0}) + \frac{1}{2}(\frac{l_0}{l})^2 - \frac{1}{2}) \tag{2.67}$$

To test to what extent the solution of the system equations of motion, obtained by direct integration, results in correct numerical energy values, the following energy residue is defined

$$R_e = W - T - U \tag{2.68}$$

For illustration purposes, we consider the bar element structure as presented in Fig. 2.4. The constitutive relationship according to Eqs. (2.19) and (2.22) has been used in the analysis.

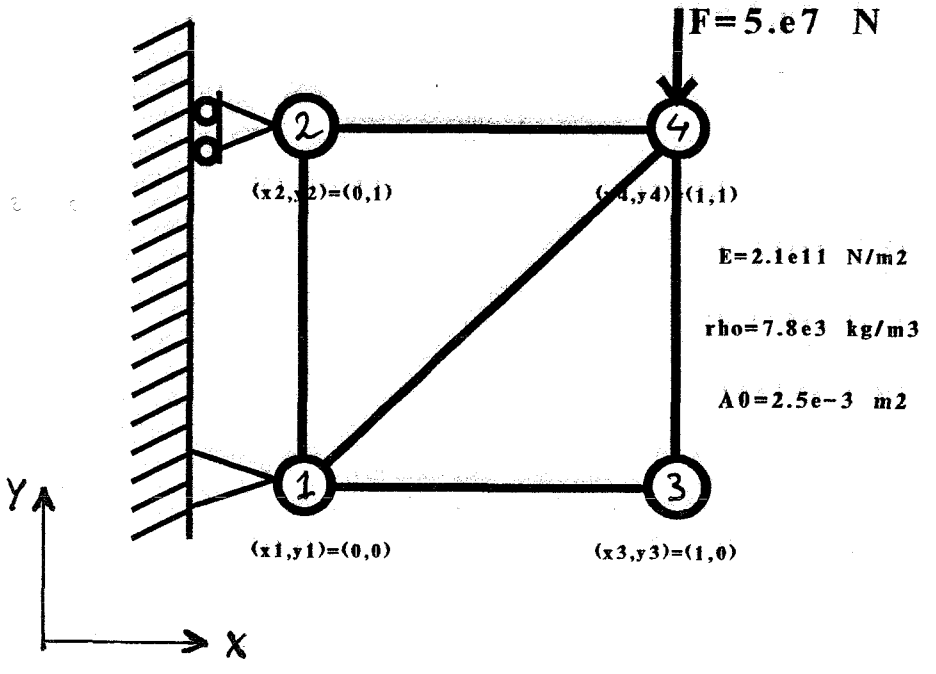


Figure 2.4: *bar element structure built up of 5 bar elements (configuration at $t = 0s$.; coordinates in meters)*

The response for the changing nodal positions as a function of time is shown in Fig. 2.5.

According to the energy balance (damping is left out of consideration), the residue for this system should be equal to 0 throughout the considered time interval of simulation (by the assumption that kinetic and potential energy in the system at $t = 0s$. equal 0). Since numerical integration is always carried out according to a user input tolerance, the residue will differ from 0. The deviation not only depends on the integration accuracy

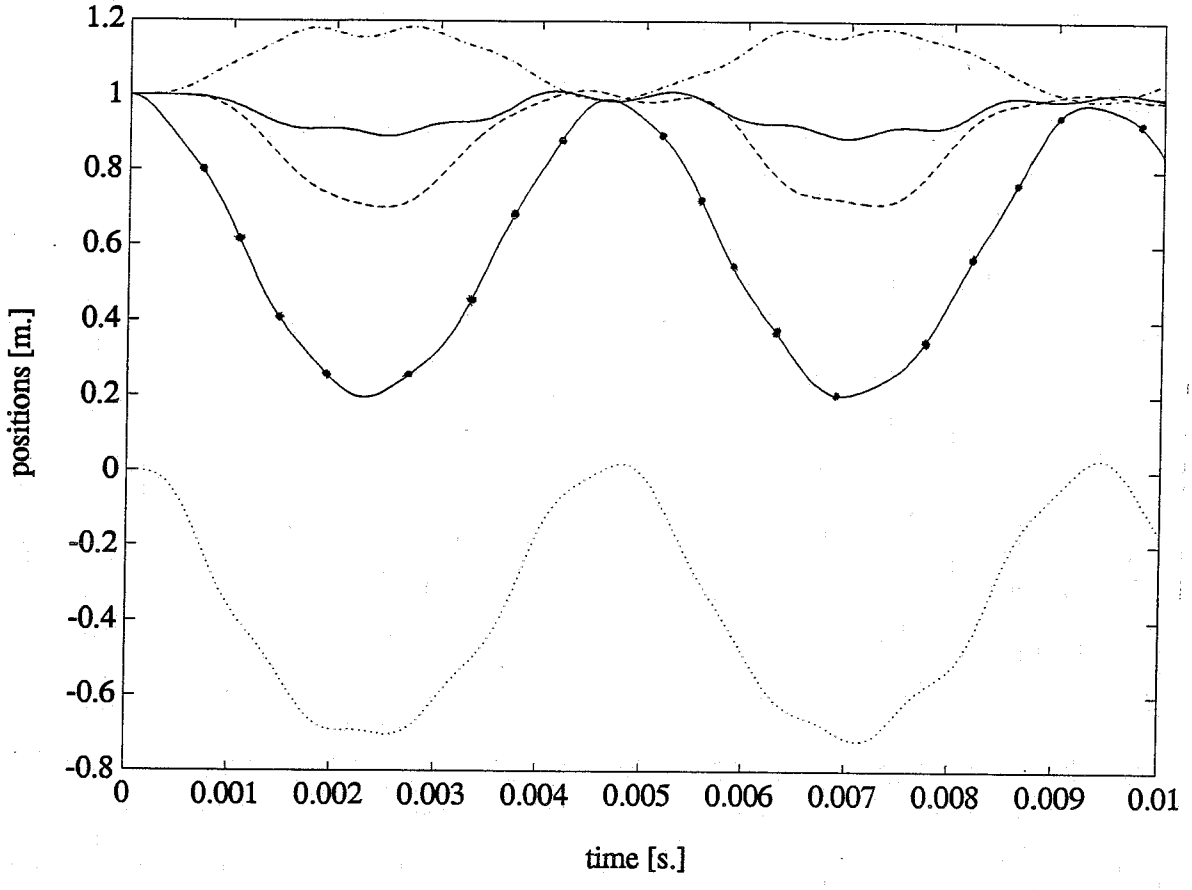


Figure 2.5: *changing nodal positions*
*x-position of node 3: - - -*
*x-position of node 4: -.-.-*
*y-position of node 2: —*
*y-position of node 3: .....*
*y-position of node 4: ——*

tolerance (Runge Kutta tolerance: *tolrk*), but also varies for different integration schemes. Fig. 2.6 shows elastic energy, kinetic energy, and external work as a function of time for the system of Fig. 2.4. Also residues for several integration schemes are plotted, e.g. classical Runge Kutta [12], Runge Kutta Fehlberg [13], and Newmark's scheme [14]. It can be concluded that the Runge Kutta methods in general (i.e. classical Runge Kutta and Runge Kutta Fehlberg) tend to have increasing integration errors (in absolute sense), whereas for Newmark's scheme, the errors remain limitted. The magnitude of the residual error can be tuned by changing the integration tolerance (compare Figs. 2.6d and 2.6e). The smaller the integration tolerance, the longer the integration computer processing time. The results of Figs. 2.6d and 2.6e were obtained by a program implemented in MS-Fortran (version 5.0 for P.C.'s), and the results of Figs. 2.6f to 2.6h were obtained by Matlab programs. Therefore the computation times needed to obtain the results as depicted in Figs. 2.6d

to 2.6h can not be compared.

Besides energy, we can also consider power of the system.

- externally applied power

$$\begin{aligned} P_w &= \dot{W}_{ext} \\ &= \underset{\sim}{f}_e \cdot \dot{\underset{\sim}{u}} \end{aligned} \tag{2.69}$$

- kinetic power

$$P_t = \sum_{i=1}^{nd} m_i \dot{\underset{\sim}{u}}_i^T \ddot{\underset{\sim}{u}}_i \tag{2.70}$$

- elastic power (compare to Eq. (2.61))

$$P_u = A_0 \frac{\sigma}{\lambda} \dot{l} \tag{2.71}$$

We can define the following power residue

$$R_p = P_w - P_t - P_u \tag{2.72}$$

In Fig. 2.7, we see that the power residue does not show an error increase, as is the case for the energy residue. The deterioration of the energy residue (see Fig. 2.6) seems to be inherent to the Runge Kutta numerical integration schemes. Since the power residue does not significantly deviate from 0, and since the magnitude of the error in energy residue can be tuned by setting the Runge Kutta integration tolerance, we need not worry about the accuracy of the direct integration solution any further.

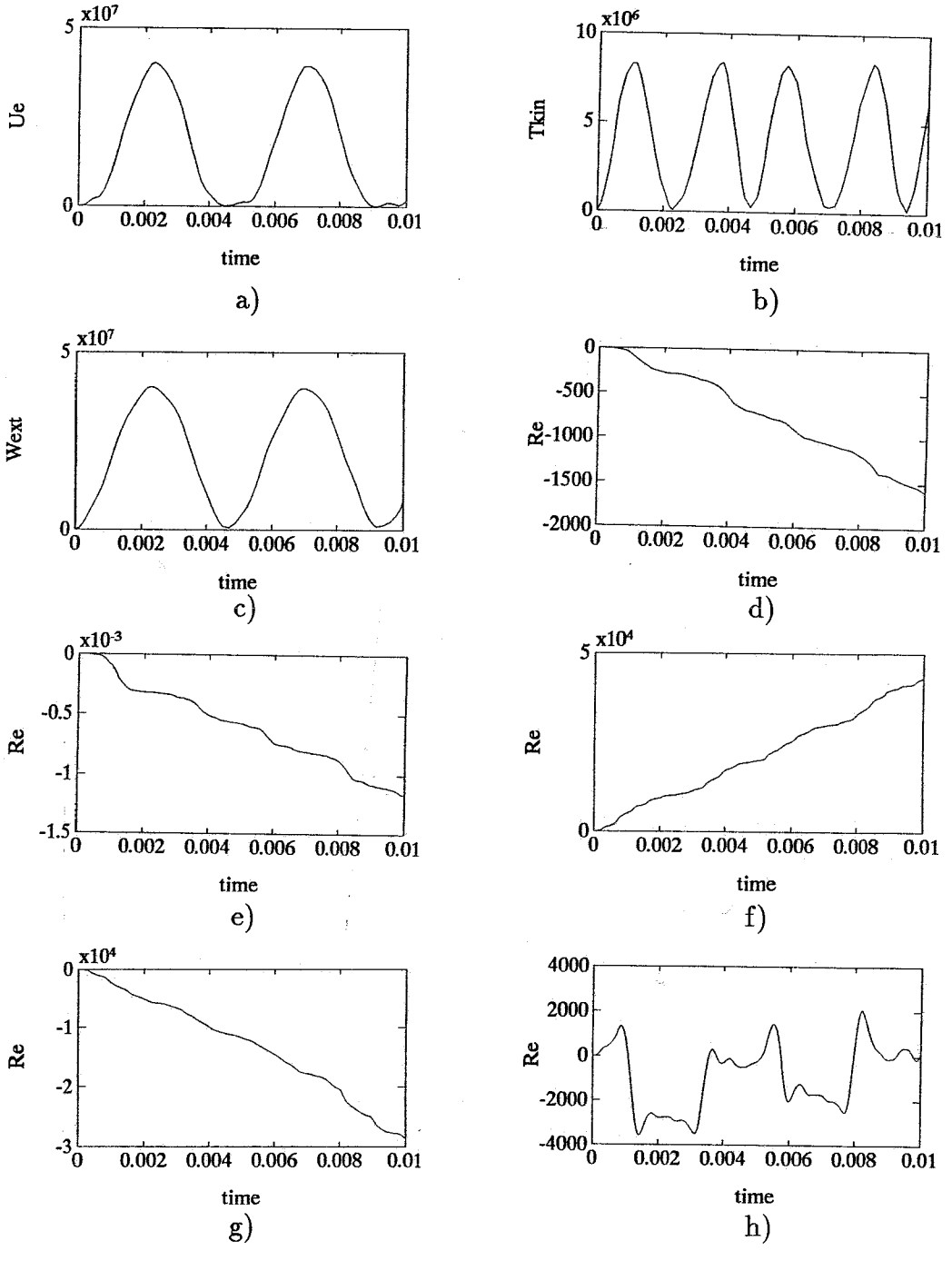


Figure 2.6: *a) elastic energy b) kinetic energy c) external work*
*Energy residues:*
*d) classical $4/5^{th}$ order Runge Kutta (tolrk=1.e-3)*
*e) classical $4/5^{th}$ order Runge Kutta (tolrk=1.e-9)*
*f) $2/3^{rd}$ order Runge Kutta Fehlberg (tolrk=1.e-3)*
*g) $4/5^{th}$ order Runge Kutta Fehlberg (tolrk=1.e-3)*
*h) Newmark ($\beta = 0.25$, $\gamma = 0.5$)*

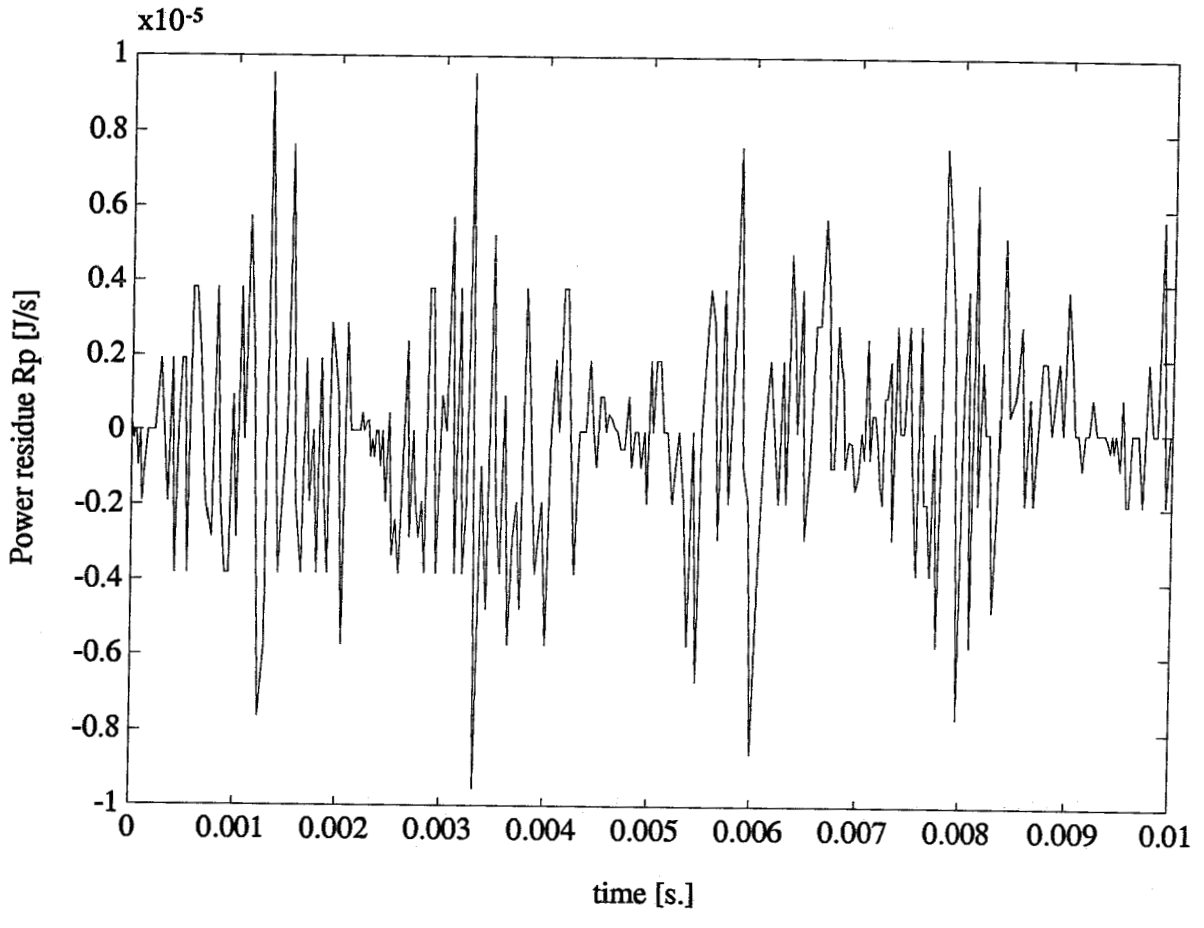


Figure 2.7: *Power residue $R_p$ for the 5 bar element structure example, 2/3$^{rd}$ order Runge Kutta Fehlberg (tolrk=1.e-3)*

# Chapter 3

# Model Reduction

## 3.1 Introduction

In nonlinear dynamics, normal modes as known from linear dynamics can not be defined, since the internal force vector is nonlinear in the system degrees of freedom. In linear dynamics, the column with internal forces corresponds to the product of the system stiffness matrix with the column of system degrees of freedom. And having the system mass matrix and stiffness matrix at one's disposal, an eigenvalue problem can be solved. With a selection of the obtained eigenmodes, the number of system degrees of freedom can be reduced. In literature on nonlinear dynamics (e.g. Refs. [6], [7], [8], [9]), one often linearizes the system equations of motion at a certain time instant in such a way, that the nonlinear internal force term transforms into a term with a stiffness matrix. The stiffness matrix in such cases is also termed 'tangent stiffness matrix' in literature. The eigenmodes that are determined from the eigenvalue problem including this tangent stiffness matrix are therefore named 'tangent modes'. Modal derivatives can be determined as a next step, but this will not be examined in this report. As has been mentioned in the introductory chapter, the reader is referred to Ref. [10] for an illustration of the use of tangent modes and modal derivatives (also applied to simple bar element structures).

In order to avoid the cumbersome determination of tangent modes and modal derivatives, an alternative strategy has been thought out [15], based on the selection of 'arbitrary modes in time' on the one hand, and nonlinear static modes on the other hand. The main idea of this strategy is to obtain 'modes' (i.e. different configurations of the system geometry) either by imposing general criteria on the solution of direct integration of the nonlinear dynamic system, possibly under other boundary loads and/or shorter integration time intervals (to reduce the effort of computing modes), or by solving the nonlinear set of algebraic equations consequent upon neglecting inertia terms and prescribing a (large) static load. A combination of these two types of modes is also possible. In the following section, the concept of arbitrary modes in time is explained. Static mode aspects are discussed in Sect. 3.3.

## 3.2 Arbitrary modes in time

In order to illustrate the idea of 'arbitrary modes in time' (or rather: 'modes' at arbitrary time instants), the system example of Fig. 2.4 is reconsidered. In Fig. 2.6, elastic and kinetic energy for the system are plotted against time. We know that elastic energy corresponds to deformation of the bar elements and kinetic energy corresponds to velocity of the masses that are lumped to the system nodes.

The maximum of the total elastic energy of the complete system is associated with a system configuration that is largely deformed. This configuration may very well be suited to use it as a 'mode' in the modal synthesis method. Fig. 3.1 shows the time instant $t^*$ of maximum elastic energy, and the deformation mode corresponding to this time instant is also shown in the figure (note: the deformation mode is scaled differently in x- and y-direction).

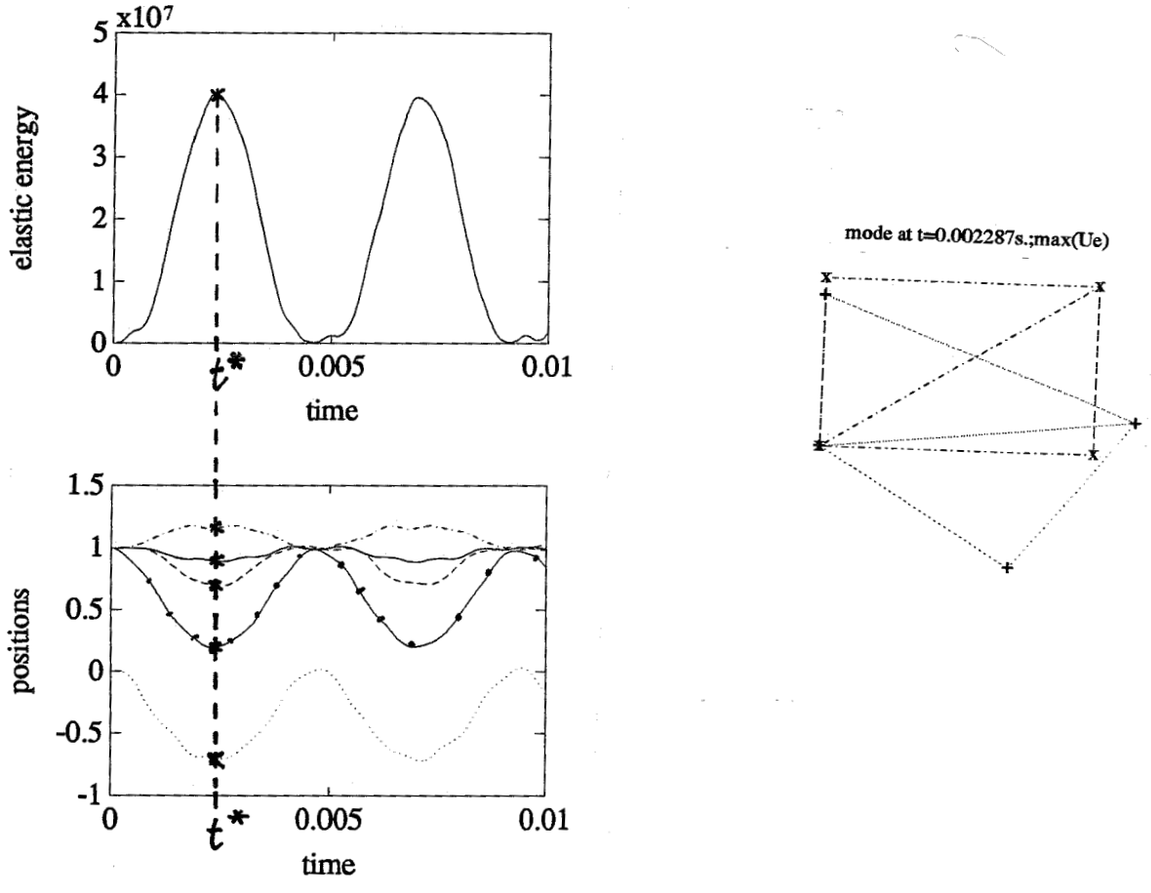


Figure 3.1: *mode corresponding to maximum elastic energy*

Similarly, we can take the configuration corresponding to the maximum kinetic energy

of the complete system as a 'mode' in the modal synthesis method. This mode will differ from the maximum elastic energy mode, and therefore might be an interesting supplement to the total set of modes that is used to reduce the system degrees of freedom. Fig. 3.2 shows the time instant $t^*$ of maximum kinetic energy, and again also the deformation mode corresponding to this time instant is shown in the figure.

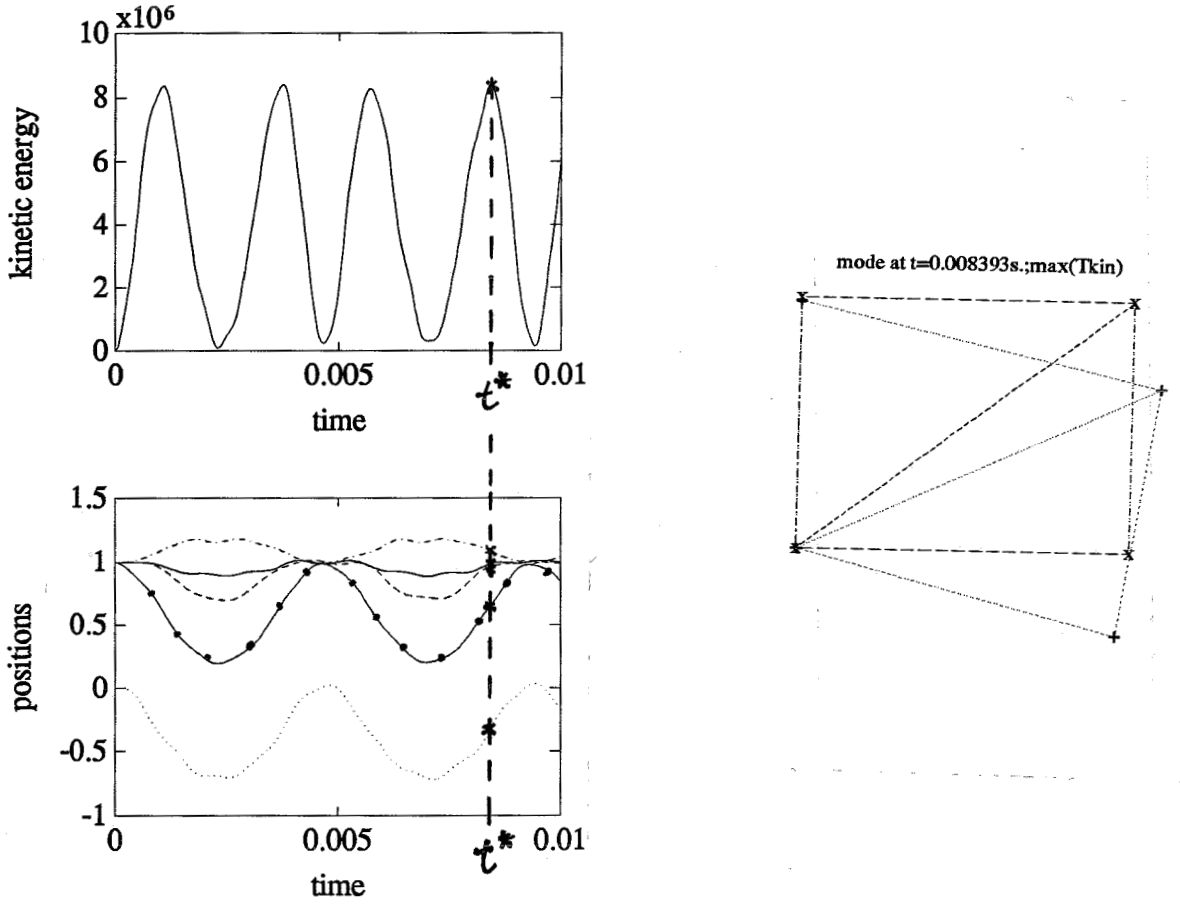


Figure 3.2: *mode corresponding to maximum kinetic energy*

Although determining this type of modes only seems to be attractive in case the direct integration of the original system does not need to be carried out (instead: execute direct integration within a shorter time domain and adapted boundary loads to determine the arbitrary modes), arbitrary modes in time will be based on the solution of direct integration of the original system in this report. A more practical or useful way of determining arbitrary modes in time is to base these modes on the solution of direct integration of a slightly different system, i.e. by directly integrating over a shorter time domain and by prescribing an impulsive load in order to generate large deformations.

## 3.3 Static modes

An alternative to the arbitrary modes in time as explained in the previous section is formed by static modes. In this case, inertia terms in the system equations of motion are neglected, and a constant static load is prescribed causing the system to deform. The nonlinear set of algebraic equations looks as follows (see Eqs. (2.43), (2.44), (2.53), (2.54), where $\underset{\sim}{f}_e$ is not time-dependent any more)

$$\underset{\sim}{f}_e - \underset{\sim}{f}_i(\underset{\sim}{u}) = \underset{\sim}{0} \tag{3.1}$$

where the internal force column is nonlinear in the displacements. A Newton-Raphson iteration process can be applied to solve this system. Eq. (3.1) can be transformed into a more common mathematical form

$$\underset{\sim}{F}(\underset{\sim}{u}) = \underset{\sim}{0} \tag{3.2}$$

In the neighbourhood of $\underset{\sim}{u}$ that makes $\underset{\sim}{F}$ zero, the function column $\underset{\sim}{F}$ may be expanded in Taylor series

$$\underset{\sim}{F}(\underset{\sim}{u} + \Delta\underset{\sim}{u}) = \underset{\sim}{F}(\underset{\sim}{u}) + \frac{\partial \underset{\sim}{F}}{(\partial \underset{\sim}{u})^T}\Delta\underset{\sim}{u} + O(\Delta\underset{\sim}{u}^2) \tag{3.3}$$

By neglecting terms of order $\Delta\underset{\sim}{u}^2$ and higher, we obtain a set of linear equations for the corrections $\Delta\underset{\sim}{u}$ that move the function column $\underset{\sim}{F}$ closer to $\underset{\sim}{0}$, namely

$$\frac{\partial \underset{\sim}{F}}{(\partial \underset{\sim}{u})^T}\Delta\underset{\sim}{u} = -\underset{\sim}{F}(\underset{\sim}{u}) \tag{3.4}$$

So, the jacobian of the function $\underset{\sim}{F}$ with respect to $\underset{\sim}{u}$ must be determined. In Appendix A, the jacobians for the different material models (see Eqs. (2.19) to (2.24)) are presented. Matrix equation (3.4) can be solved by LU-decomposition. The corrections are then added to the solution vector,

$$\underset{\sim}{u}^{new} = \underset{\sim}{u}^{old} + \Delta\underset{\sim}{u} \tag{3.5}$$

and the process is iterated to convergence. In order to enable convergence to the correct root of the nonlinear system, the incremental load approach [16] is appropriate. Small load increments reduce the total number of iterations required for convergence per increment.

## 3.4 Reduction criteria

Several criteria can be handled to make a choice for the modes that are used to reduce the number of original system degrees of freedom (say $N$). Any combination of modes will do to reduce the system, provided that the modes are mutually independent. And, of course, the one set of modes yields better results for the reduced system solution than the other.

Dependency between modes appears quite obviously, since the matrix $\underline{M}^r$ is singular then, and inversion as in Eq. (2.49) is not possible in that case.

The ideas to determine modes for the modal synthesis method, as presented in Sections 3.2 and 3.3 have been implemented in a computer program. In the following, some proposals for mode selection are presented. At first, the screen output of the implemented interactive program is shown. After that, some information on the contents of the screen output is provided.

When direct integration of the original (or slightly different) system has been completed, the solution can be used to compute system energies. The following lines will appear on the screen then:

```
>> dcrit
System energies are computed ...

Select dynamic "mode(s)", i.e. configuration(s) corresponding to:
1. minimum strain energy of complete system
2. maximum strain energy of complete system
3. minimum kinetic energy of complete system
4. maximum kinetic energy of complete system
5. minimum external work of complete system
6. maximum external work of complete system
7. all unique maximum values of the system d.o.f.-s
8. half & full time interval of the largest strain
   (first & very largest, resp)
9. neglecting mass, i.e. static mode(s)

 Make your choice(s)
```

When the system energies have been computed, minima and maxima of the various types of energy can be determined. The corresponding system configurations may be regarded as modes, which can be gathered in the reduction matrix $\underline{\Phi}$ (see Eq. (2.39)).

The seventh option checks the maximum of the absolute value of each nodal displacement; if the time corresponding to this maximum has not been selected for previously checked displacements, then the system configuration at that time instant is chosen as a mode in $\underline{\Phi}$.

The eighth option calculates two modes. The first mode is based on the *first* strain maximum of an arbitrary bar element in the system; the corresponding time is divided by two and the system configuration at that 'half time' is taken as a mode. The time is divided by two in order to let the first mode differ from the second mode. The second mode is obtained by calculating the *largest* strain maximum of an arbitrary element in the system throughout the complete integration time interval.

The ninth option enables the selection of static modes. The static analysis must have been completed before arriving at the above menu. The user is supposed to have the static

mode data in a prepared file, which can be read in by the program.

Several combinations of the above options are also possible. However, the less modes one selects, the less computer time is needed for the reduced system integration. Probably, fewer modes will also introduce larger errors. These errors can be reduced though, by selecting the right modes that have large influence on the system response.

# Chapter 4

# Some Numerical Results

## 4.1 Structure consisting of 21 bar elements

The examples in this report are not intended to test whether results are physically meaningful, but rather to compare the *reduced* system solution to the *complete* system solution.

In this section, we will focus on the category of 'arbitrary modes in time'. As already mentioned at the end of Chapter 3, the choices for the selected sets of modes are arguable. We consider the 21 bar element structure as depicted in Fig. 4.1. The system has 12 nodes with 2 degrees of freedom at each node. Three degrees of freedom are suppressed by boundary conditions, so 21 degrees of freedom result for the total system.

In the analysis, we use the constitutive relation according to Eqs. (2.19) and (2.22). Furthermore, we use a lumped mass approach (see Eq. (2.41)). A constant external force $F$ acts on the structure at node 12. In a static analysis, the system would deform to a static equilibrium. In a dynamic analysis though, the system will vibrate around that equilibrium configuration (damping is not considered). The energies in the system as a function of time are shown in Fig. 4.2.

Results for the dynamic analysis are shown in Appendix B. Several reduction mode sets are tried in order to examine their influence on the reduced system solution. The modes that are used in the modal synthesis are shown in Appendix B. Table 4.1 provides a survey of the four reduced simulations that have been executed.

In Appendix B, we see that the second simulation shows better results than the first simulation. The influence of the mode corresponding to $max(U)$ is larger than the mode

| simulation | used mode(s) | option in program | results shown in Sect. |
|---|---|---|---|
| 1 | $max(T)$ | 4 | B.1 |
| 2 | $max(U)$ | 2 | B.2 |
| 3 | $max(T), max(U)$ | 2,4 | B.3 |
| 4 | $max(T), max(U), max(\lambda)$ | 2,4,8 | B.4 |

Table 4.1: Used sets of arbitrary modes in time.

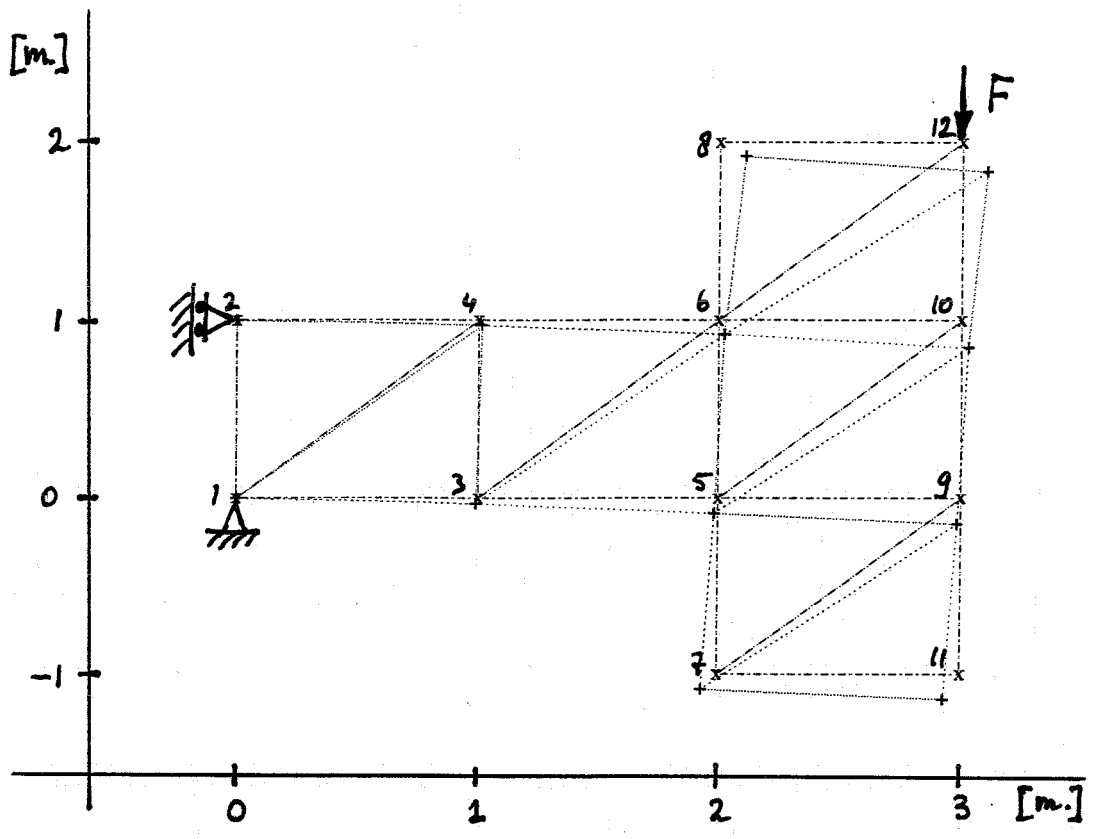


Figure 4.1: *21 bar element structure* ($E$ = *2.1e11* $\frac{N}{m^2}$, $A_0$ = *2.5e-3* $m^2$, $\rho_0$ = *7.8e3* $\frac{kg}{m^3}$, $F$ = *5.e6 N*)

corresponding to $max(T)$. This may seem trivial, since potential energy is more associated with deformations than kinetic energy, but it also points out that the reduced solution can be improved by taking a different mode. The reduced solution can also be examined for the case where the modes of the first two simulations are combined. In Appendix B.3, we can see that the reduced solution is improved again (with respect to both first simulations). Apparently, these two modes supplement each other quite well. By adding a third mode (the second mode obtained by the eighth option as described in Sect. 3.4), the solution only improves marginally. It appears that this mode does not add much information to the combination of the other two modes, probably due to the similarity between the second and third mode.

A final remark must be made on gains in computation times by the modal synthesis method. Integration of the complete and the reduced system equations of motion is carried out by Runge Kutta integration schemes with variable time step. By reducing the system and taking the modal coordinates as new degrees of freedom, the new system may need more (and smaller) time steps over the integration time interval. The number of (derivative)

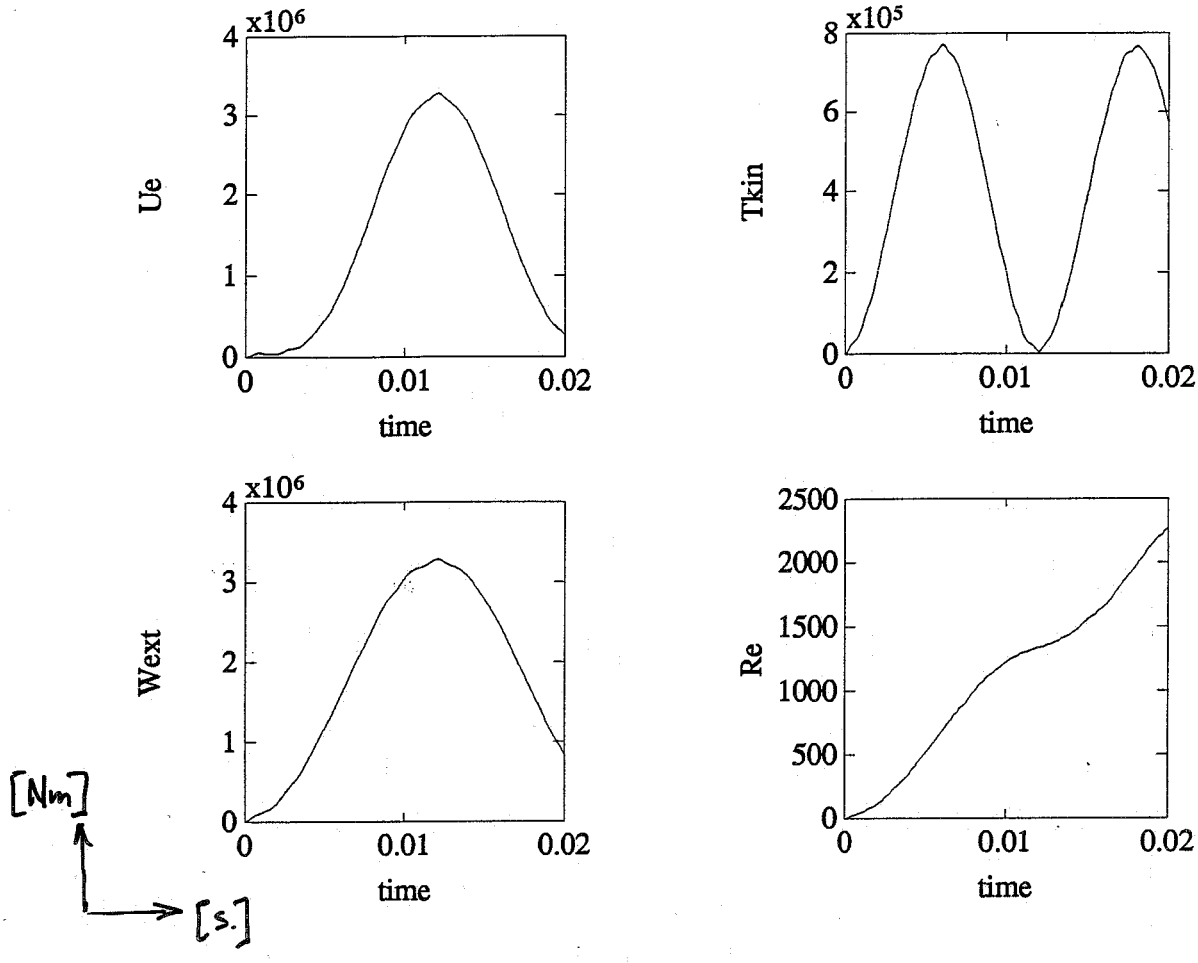


Figure 4.2: *system energies for the 21 bar element structure*

function evaluations will also increase then, so that the gain in total computation time decreases. E.g. in the fourth simulation, the original 21 degrees of freedom are reduced to 3 modal coordinates. The number of floating point operations per function evaluation turns out to be reduced by about 35 percent. But since more function evaluations are needed, the total number of floating point operations for the complete simulation remains about the same! This numerical aspect needs a thorough study and further optimization.

## 4.2 Structure consisting of 101 bar elements

This section focusses on the category of static modes. Again, as in the previous section, the choices for the selected sets of modes are arguable. Static modes are based on static loads that act on the system. In order to let static modes be useful in a dynamic analysis, the engineer must be able to determine dominant forces and modes, based on experience.

The example in this section is intended to show that a system with many degrees of freedom can be reduced by only a few static modes and yet provide reasonable results. The idea existed simply to increase the static forces that act on the nonlinear system by a

scaling factor and determine the corresponding static modes, and to examine whether use of these few modes enable a proper simulation of the dynamic system in a reduced form.

Bathe et al.(1975, see Ref. [17]) describe an example on large strain dynamic analysis of a rubber sheet with a hole (see Fig. 4.3). It concerns a plane stress analysis with the purpose to test the capability of predicting static and dynamic large strain response. The material of the rubber sheet is assumed to be of Mooney-Rivlin type.

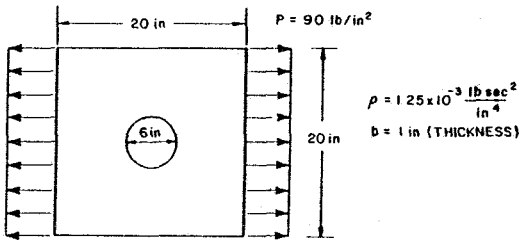


Figure 4.3: *rubber sheet with a hole (from Bathe et al. (1975))*

The specific material constants used for the hyperelastic incompressible material were $c_1 = 25[psi]$, $c_2 = 7[psi]$. The units from Bathe's article have been converted to SI-units in this report, so $c_1 = 1.72e5[Pa]$, $c_2 = 0.48e5[Pa]$. The material density in the reference configuration is $\rho_0 = 1.1e3[\frac{kg}{m^3}]$. Since Bathe uses 4- or 8-node 2D plane stress elements, his results can not be compared to results based on bar elements, which was not the intention of this example anyway. The example of Bathe et al. has been chosen here, because it is an example from one of the few articles in literature that describes large deformations in a dynamic analysis. Where Bathe et al. take one inch for the plane stress element thickness, in this report the cross section area of each bar in the reference configuration, $A_0$, is taken equal to $2.5e-3[m^2]$. Only a fourth part of the geometry needs to be modelled (see Fig. 4.4).

The constant force value P in Fig. 4.4 is equal to $667.2[N]$ in the dynamic analysis. Three static modes have been determined, i.e. for $P = 333.6[N], 500.4[N], 667.2[N]$, respectively. The 3 static modes that are used to reduce the system of 72 degrees of freedom (the system has 42 nodes with 2 d.o.f. at each node, and 12 degrees of freedom are suppressed) are depicted in Fig. 4.5.

Results of the simulation are shown in Fig. 4.6. Comparison of the computation times for complete system integration and reduced system integration learns that integrating the reduced system with 3 unknowns is 2.25 times as fast as integrating the original system with 72 unknowns.

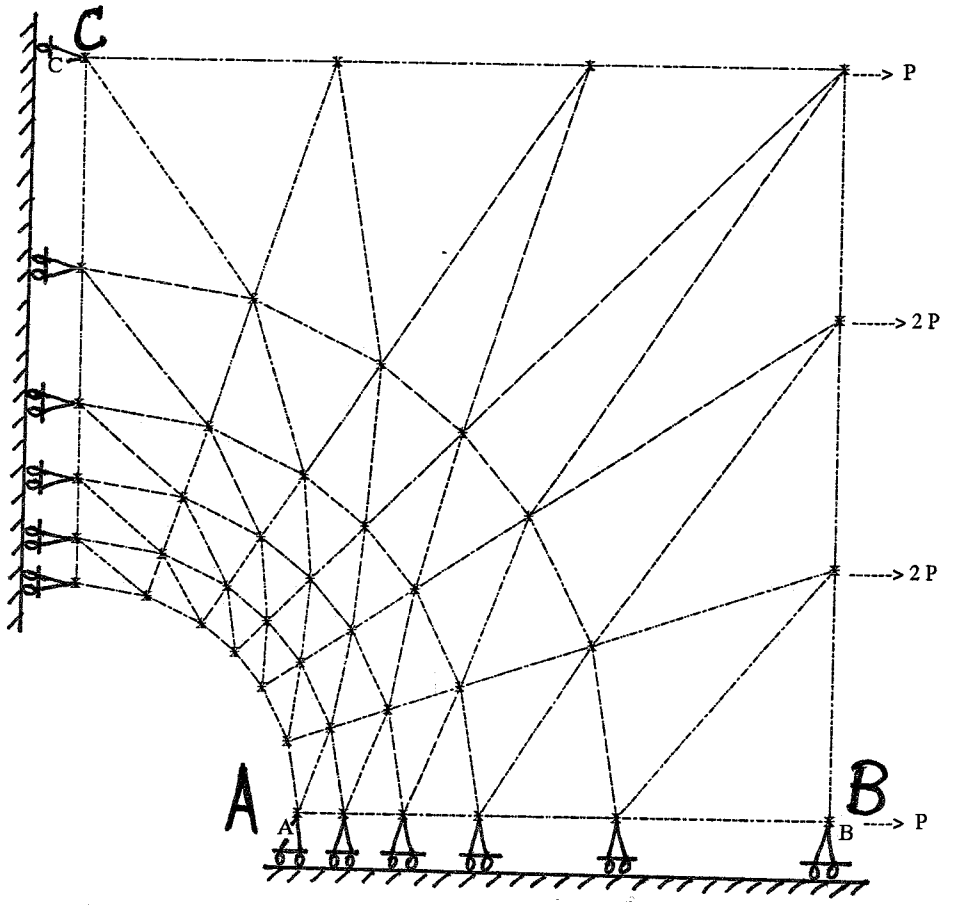


Figure 4.4: *finite element model of rubber sheet with a hole, consisting of 101 bar elements (lumped mass approach)*

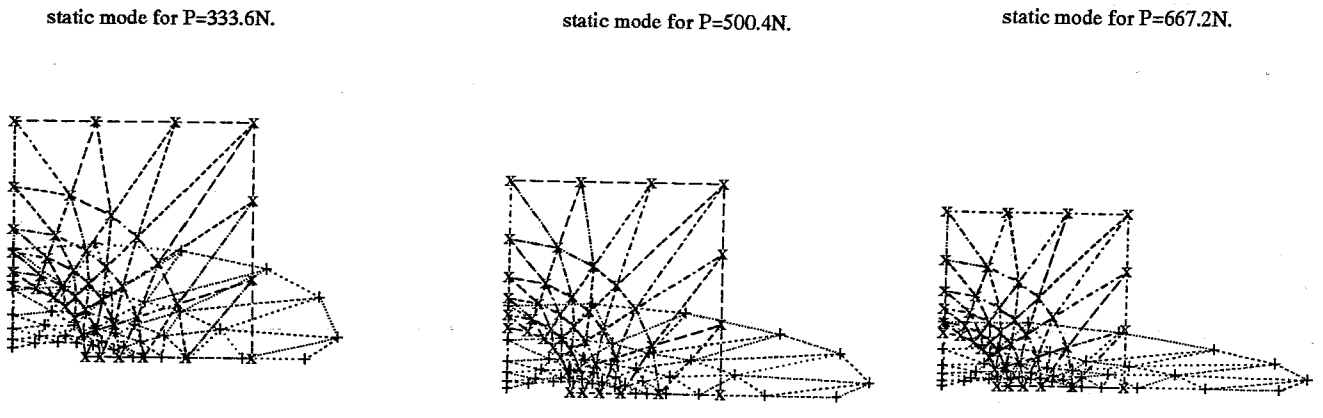


Figure 4.5: *static modes used in the modal synthesis method*

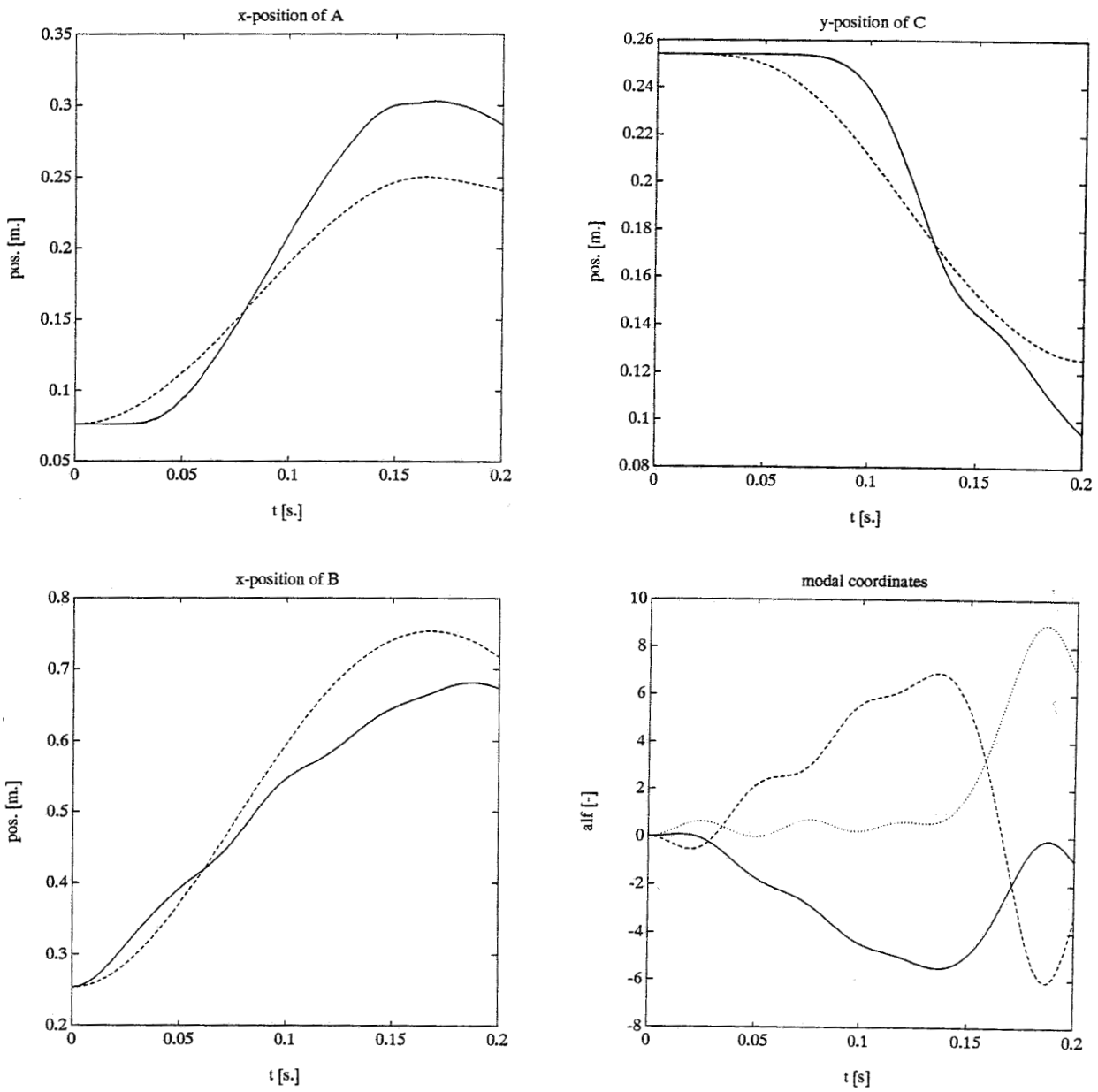


Figure 4.6: *simulation results: positions of nodes a, b, and c*
*— direct integration of original system*
*- - direct integration of reduced system*
*and modal coordinates as a function of time:*
*— modal coordinate corresponding to static mode for* $P = 333.6[N]$
*- - modal coordinate corresponding to static mode for* $P = 500.4[N]$
*... modal coordinate corresponding to static mode for* $P = 667.2[N]$

# Chapter 5

# Conclusions and Recommendations

## 5.1 Conclusions

The modal synthesis method, applied to deformable bodies in multibody systems, is an interesting method regarding the small number of degrees of freedom that is involved, and, consequently, the limited computation times. The idea of using the modal synthesis method in large deformation dynamics has been tested for bar element systems. After implementation of the ideas as presented in Chapters 2 and 3, it can be concluded that software tools are available, so that more numerical try outs can be carried out. More simulations are needed in order to find out which are the best mode selection criteria to obtain reduced integration solutions of best quality with as less effort as possible.

'Arbitrary modes in time' are based on the solution of direct integration of the original system thus far, and reasonable results can be obtained for the reduced integration solution, although there is need for improvement in the reduced solution. By basing these modes on maxima or minima of energy terms of the complete dynamic system, general ways of creating these modes have been developped, which can be automated quite easily. The 21 bar element structure has been reduced with several combinations of modes. The reduced solution can be improved without too much effort: in case two modes are selected (based on maxima in potential and kinetic energy) instead of only one of these modes, an obvious improval in the reduced solution can be noticed. Adding other modes to the mode set may not always be efficient, as shown in the 21 bar element example.

The advantage of using static modes is that no eigenvalue problem needs to be solved as compared to the strategy of determining tangent modes and modal derivatives, and an advantage with respect to the approach of 'arbitrary modes in time' is that no direct integration needs to be done *a priori*. Instead, a Newton-Raphson iteration process must be executed in order to obtain static modes. An efficient selection of a set of these kinds of modes is problem dependent, and can therefore hardly be automated. The engineer must rely on his experience when selecting this type of modes. The 101 bar element example shows that a nonlinear dynamic problem can be reduced by static modes in the modal synthesis method. Qualitatively, the reduced system solution shows the same

behaviour as the complete system solution. Quantitatively, the reduced system solution needs improvement. Static modes may also be combined with arbitrary modes in time, which is an existing option in the available software already.

As far as the reduction of computation times is concerned, further optimization is appropriate. The Runge Kutta integration scheme with variable time step may need more time steps and function evaluations in case the system equations are reduced. Then again, a gain in total computation time can be achieved by using the advantage of less floating point operations for each function evaluation in case the system is reduced.

## 5.2 Recommendations

Several recommendations for future research can be thought of.

- Of course, more numerical experiments are needed to get a better impression of the meaning and usefulness of criteria for arbitrary modes in time.
- So far in this report, arbitrary modes in time are based on calculations on the solution of direct integration of the complete system. It is not practical to solve the complete system first; an interesting option may be to consider different boundary loads and shorter integration time intervals to determine the arbitrary modes (e.g. use dynamic pulse loads to generate large deformations). However, it must be remarked that this approach would also make the selection of modes problem dependent (and more difficult to automate).
- Updating of modes (static or arbitrary modes in time) is also possible. As soon as the approximate solution deviates too much from the exact solution, to be checked by defining an 'equation-of-motion-residue' (see e.g. Ref. [10]), the set of modes can be updated. Although, it must be mentioned that de Jongh in Ref. [10] did not obtain very successful results using updating of tangent modes (due to presumed transformation errors at each update, i.e. when transforming the nonreduced accelerations to reduced accelerations). The idea of updating modes should not totally be rejected though.
- Consider other types of elements, e.g. beam elements, 3D-solid elements, or other elements that are of interest to model deformable bodies in multibody systems.
- Structural damping, left out of consideration in this report, can also be taken into account. It can be investigated what influence damping has on the results obtained by the modal synthesis method.
- The fitting of the structural dynamics part into the multibody dynamics part must finally be taken care of, i.e. superpose displacements as a rigid body to the displacements due to deformation as considered in this report.

# Bibliography


[1] W.P. Koppens. *The Dynamics of Systems of Deformable Bodies.* PhD thesis, Eindhoven University of Technology, 1989.

[2] J.S. Przemieniecki. *Theory of Matrix Structural Analysis.* McGraw-Hill, 1968.

[3] L. Vu-Quoc. *Dynamics of Flexible Structures Performing Large Overall Motions: a Geometrically-Nonlinear Approach.* PhD thesis, University of California, Berkeley, 1986.

[4] J.C. Simo and L. Vu-Quoc. On the dynamics of flexible beams under large overall motions — the plane case: part 1. *Journal of Applied Mechanics*, 53:849–854, 1986.

[5] DADS Revision 5.0. *DADS Flexible Bodies Theoretical Manual.* Computer Aided Design Software Incorporated, 1987.

[6] S.R. Idelsohn and A. Cardona. Recent advances in reduction methods in nonlinear structural dynamics. In M. Petyt and H.F. Wolfe, editors, *Proceedings of the Second International Conference on: Recent Advances in Structural Dynamics, vol. II*, pages 475–482, University of Southampton, England, 1984.

[7] S.R. Idelsohn and A. Cardona. A reduction method for nonlinear structural dynamic analysis. *Computer Methods in Applied Mech. and Eng.*, 49:253–279, 1985.

[8] S.R. Idelsohn and A. Cardona. Computational strategies for nonlinear and fracture mechanics problems. *Computers & Structures*, 20(1-3):203–210, 1985.

[9] C. Chang and J.J. Engblom. Nonlinear dynamical response of impulsively loaded structures: a reduced basis approach. *AIAA Journal*, 29(4):613–618, 1991.

[10] J. de Jongh. *A Reduction Method for Nonlinear Dynamic Systems.* Technical Report WFW-report 92.102, Eindhoven University of Technology, Computational and Experimental Mechanics Group, Department of Mechanical Engineering, 1992.

[11] P.J.G. Schreurs. Personal notes. 1991. Department of Mechanical Engineering, Eindhoven University of Technology.

[12] W.H. Press, B.P. Flannery, S.A. Teukolsky, and W.T. Vetterling. *Numerical Recipes: the Art of Scientific Computing.* Cambridge University Press, USA, 1989.

[13] G.E. Forsythe, M.A. Malcolm, and C.B. Moler. *Computer Methods for Mathematical Computations.* Prentice-Hall, Inc. Englewood Cliffs, New Jersey, 1977.

[14] K.J. Bathe and E.L. Wilson. *Numerical Methods in Finite Element Analysis.* Prentice-Hall, Inc. Englewood Cliffs, New Jersey, 1976.

[15] A.A.H.J. Sauren and W.P. Koppens. Personal communication. 1991. Department of Mechanical Engineering, Eindhoven University of Technology, and TNO Road-Vehicles Research Institute, Delft.

[16] O.C. Zienkiewics and R.L. Taylor. *The Finite Element Method, Vol.1: Basic Formulation and Linear Problems, Vol.2: Solid and Fluid Mechanics; Dynamics and Non-linearity.* McGraw-Hill Book Company, 1989.

[17] K.J. Bathe, E. Ramm, and E.L. Wilson. Finite element formulations for large deformation dynamic analysis. *Int. J. for Num. Methods in Eng.*, 9:353–386, 1975.

# Appendix A

# Newton-Raphson Iteration Jacobians

In general, the jacobian $\underline{K} = \frac{\partial \underset{\sim}{F}}{(\partial \underset{\sim}{u})^T}$ (see Eq. (3.4)) has the following form

$$\underline{K} = \begin{bmatrix} \underline{k} & -\underline{k} \\ -\underline{k} & \underline{k} \end{bmatrix} \tag{A.1}$$

with

$$\underline{k} = \begin{bmatrix} k_{11} & k_{12} \\ k_{21} & k_{22} \end{bmatrix} \tag{A.2}$$

where $k_{21} = k_{12}$ (due to symmetry).
For the constitutive relation according to Eqs. (2.19) and (2.20), $\underline{k}$ has the following form

$$\begin{aligned} k_{11} &= \frac{EA_0(l-l_0)}{l^2}(n_{12}^2 - n_{11}^2) + \frac{EA_0}{l}n_{11}^2, \\ k_{12} &= \frac{EA_0(l-l_0)}{l^2}(-2n_{11}n_{12}) + \frac{EA_0}{l}n_{11}n_{12}, \\ k_{22} &= \frac{EA_0(l-l_0)}{l^2}(n_{11}^2 - n_{12}^2) + \frac{EA_0}{l}n_{12}^2, \end{aligned} \tag{A.3}$$

and for the constitutive relation according to Eqs. (2.19) and (2.21)

$$\begin{aligned} k_{11} &= \frac{EA_0(l^2-l_0^2)}{2l_0l^2}(n_{12}^2 - n_{11}^2) + \frac{EA_0}{l_0}n_{11}^2, \\ k_{12} &= \frac{EA_0(l^2-l_0^2)}{2l_0l^2}(-2n_{11}n_{12}) + \frac{EA_0}{l_0}n_{11}n_{12}, \\ k_{22} &= \frac{EA_0(l^2-l_0^2)}{2l_0l^2}(n_{11}^2 - n_{12}^2) + \frac{EA_0}{l_0}n_{12}^2, \end{aligned} \tag{A.4}$$

and for the constitutive relation according to Eqs. (2.19) and (2.22)

$$\begin{aligned} k_{11} &= \frac{EA_0 l_0 \ln(\frac{l}{l_0})}{l^2}(n_{12}^2 - n_{11}^2) + \frac{EA_0 l_0}{l^2} n_{11}^2, \\ k_{12} &= \frac{EA_0 l_0 \ln(\frac{l}{l_0})}{l^2}(-2n_{11}n_{12}) + \frac{EA_0 l_0}{l^2} n_{11}n_{12}, \\ k_{22} &= \frac{EA_0 l_0 \ln(\frac{l}{l_0})}{l^2}(n_{11}^2 - n_{12}^2) + \frac{EA_0 l_0}{l^2} n_{12}^2. \end{aligned} \tag{A.5}$$

For the Mooney-Rivlin constitutive relation (according to Eq. (2.24)), $\underline{k}$ results as

$$\begin{aligned} k_{11} &= \frac{A_0}{l_0}\left\{\left[c_1(1+2(\frac{l_0}{l})^3) + c_2 3(\frac{l_0}{l})^4\right] n_{11}^2 + \left[c_1(1-(\frac{l_0}{l})^3) + c_2(\frac{l_0}{l} - \frac{l_0}{l})^4)\right] n_{12}^2\right\}, \\ k_{12} &= \frac{A_0}{l_0}\left\{c_1 3(\frac{l_0}{l})^3 + c_2(-\frac{l_0}{l} + 4(\frac{l_0}{l})^4\right\} n_{11}n_{12}, \\ k_{22} &= \frac{A_0}{l_0}\left\{\left[c_1(1+2(\frac{l_0}{l})^3) + c_2 3(\frac{l_0}{l})^4\right] n_{12}^2 + \left[c_1(1-(\frac{l_0}{l})^3) + c_2(\frac{l_0}{l} - \frac{l_0}{l})^4)\right] n_{11}^2\right\}. \end{aligned} \tag{A.6}$$

In case $c_2 = 0$, the result for $\underline{k}$ according to the Neo-Hookean constitutive relation (according to Eq. (2.23)) appears.

The above equations (A.3) to (A.6) have been implemented in a software program. Note that Eqs. (A.3) to (A.5) can quite easily be transformed into Eqs. (B.30) to (B.32) in Ref. [10], by the following geometric relation

$$n_{11}^2 + n_{12}^2 = 1. \tag{A.7}$$

# Appendix B

# Results for the 21 Bar Element Structure

## B.1 Simulation 1

mode at t=0.006056s.;max(Tkin)

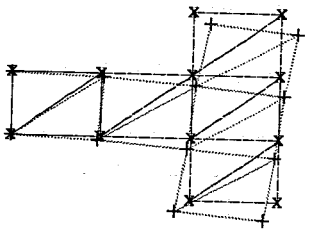

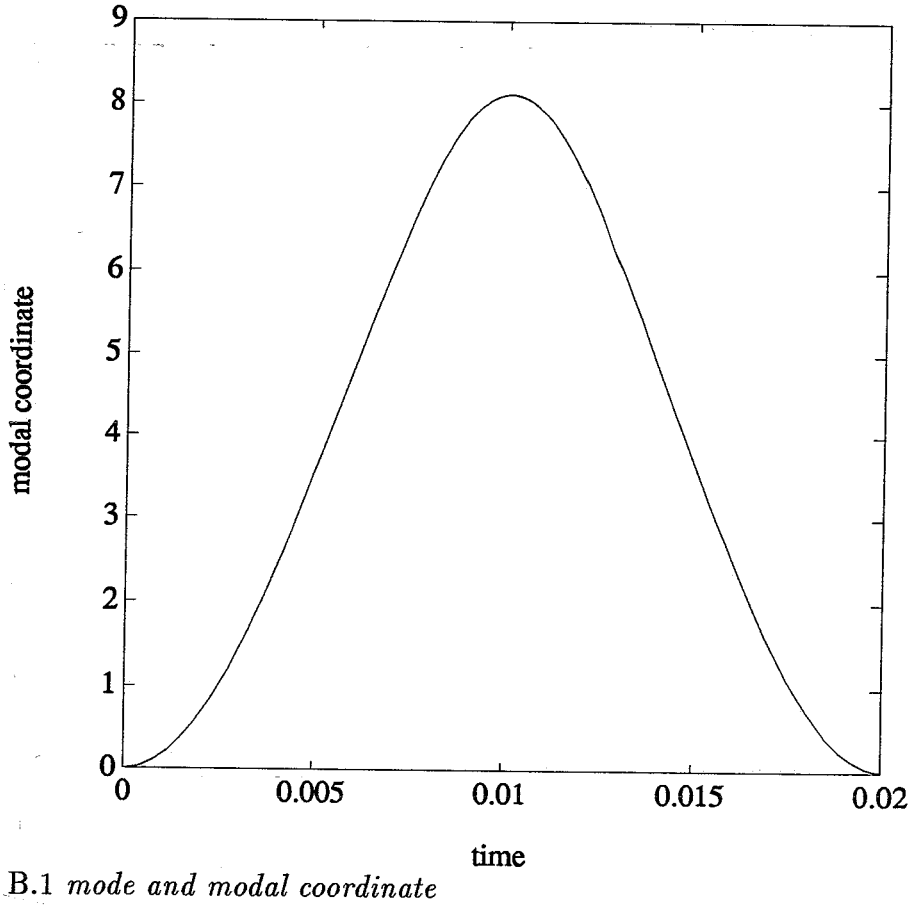


Fig. B.1 *mode and modal coordinate*

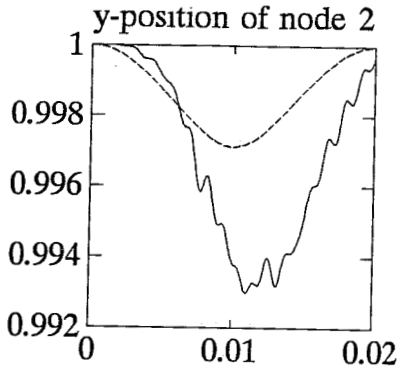


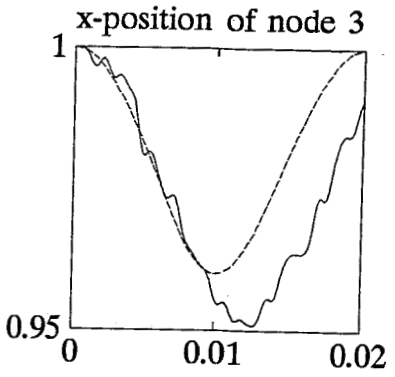


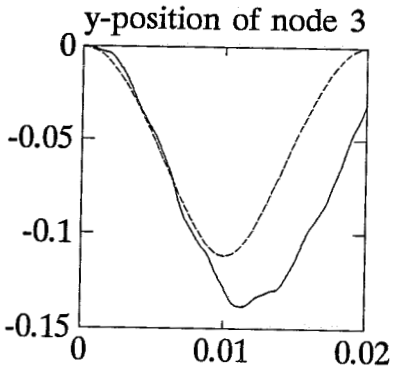


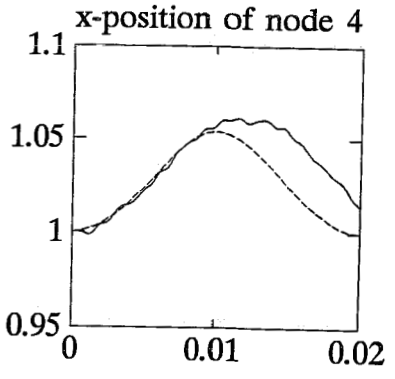


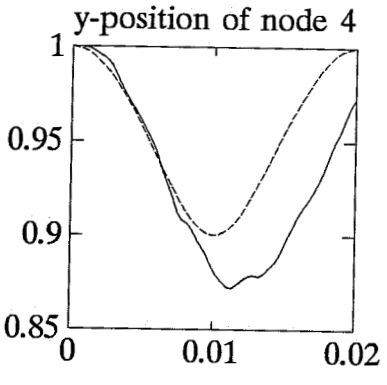


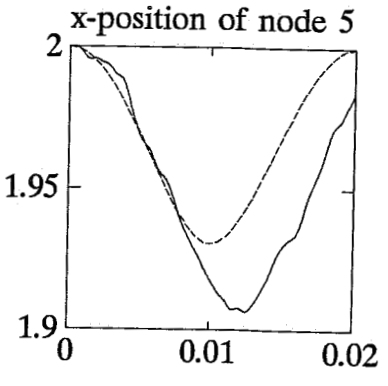


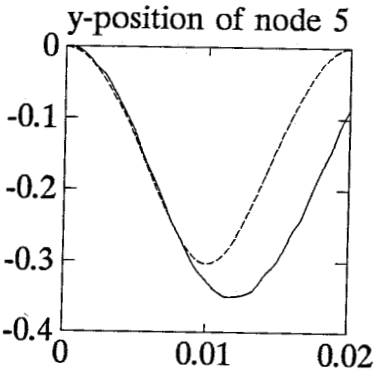


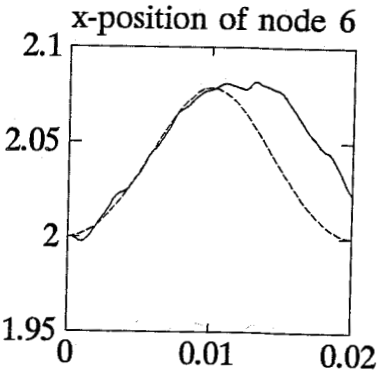


Fig. B.2 — *direct integration of original system*
*- - direct integration of reduced system*

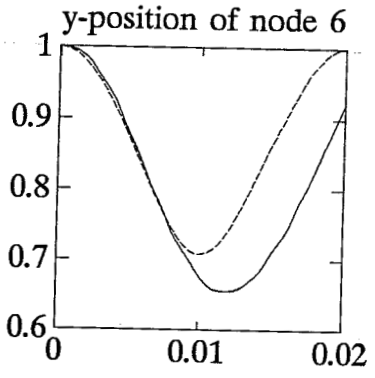


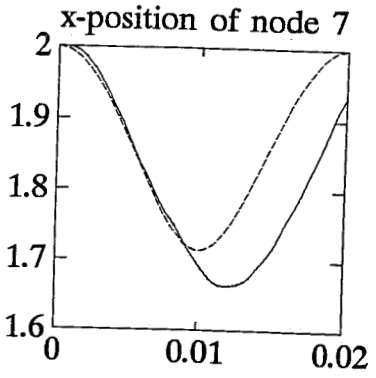


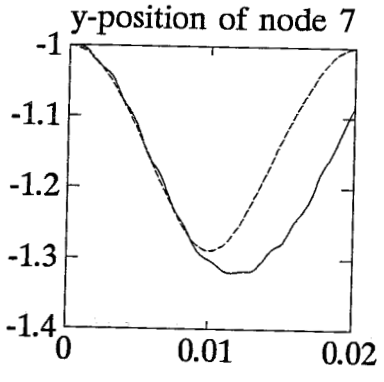


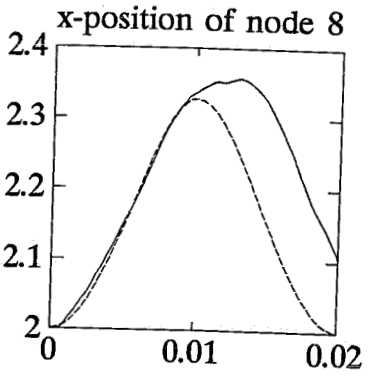


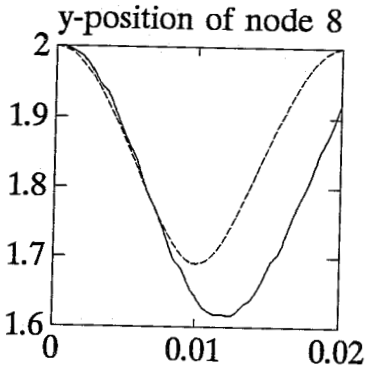


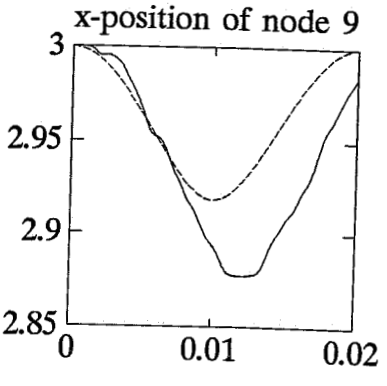


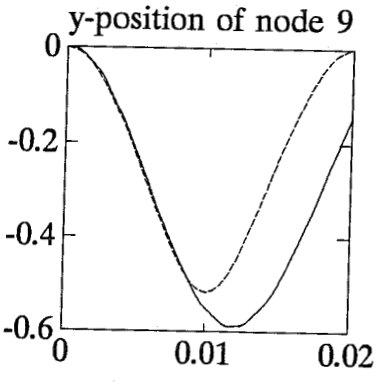


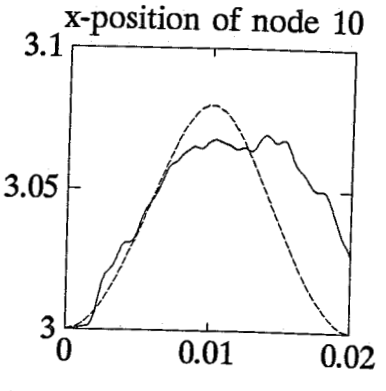


Fig. B.3 — *direct integration of original system*
*- - direct integration of reduced system*

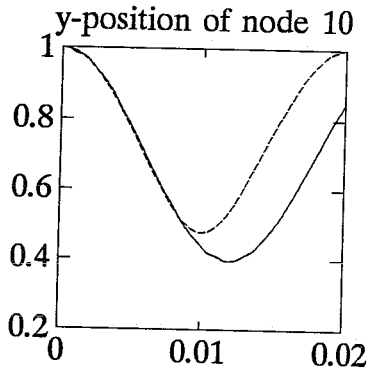


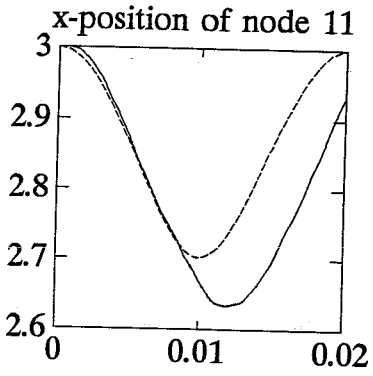


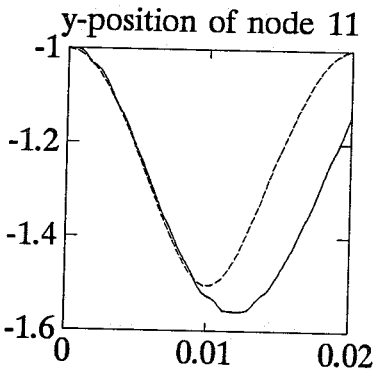


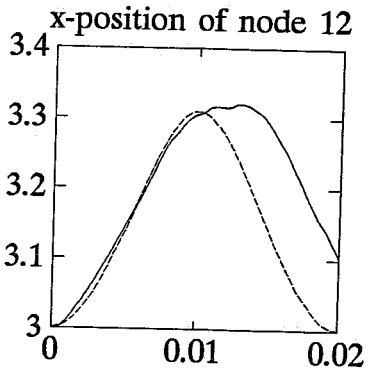


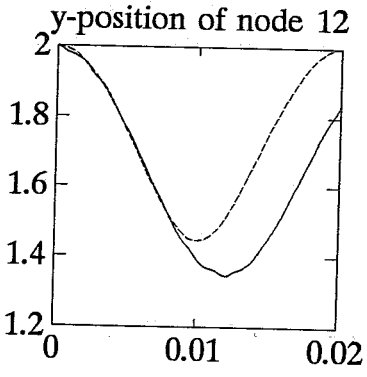


Fig. B.4 — *direct integration of original system*
*- - direct integration of reduced system*

## B.2 Simulation 2

mode at t=0.01207s.;max(Ue)

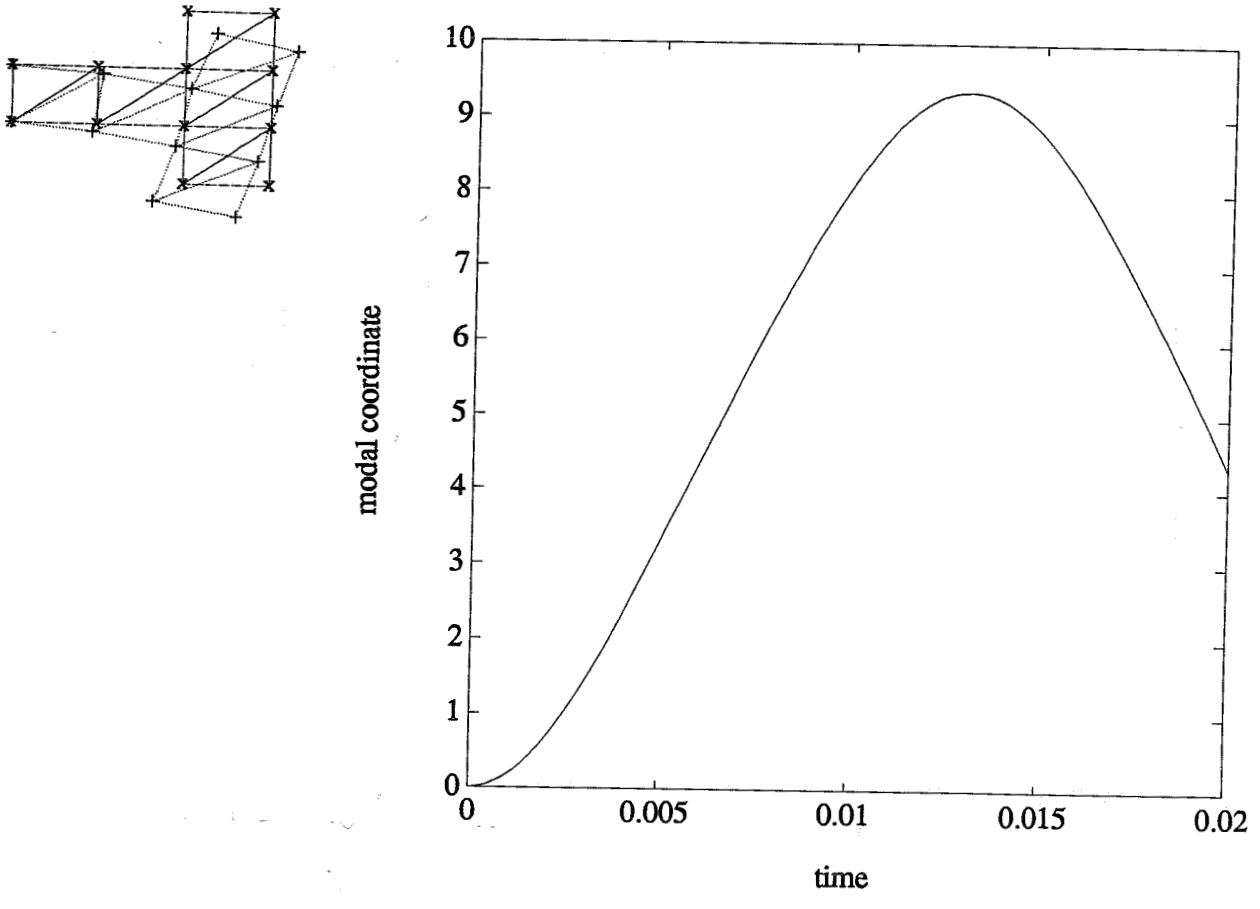


Fig. B.5 *mode and modal coordinate*

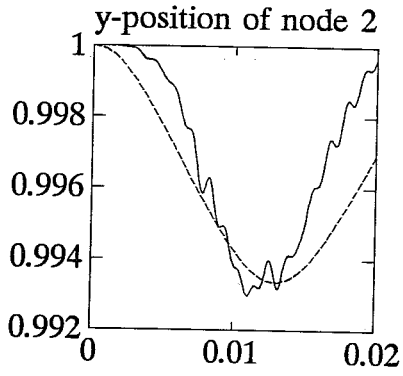


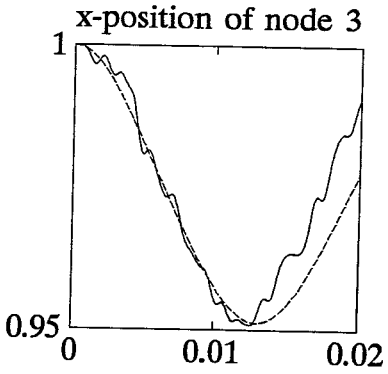


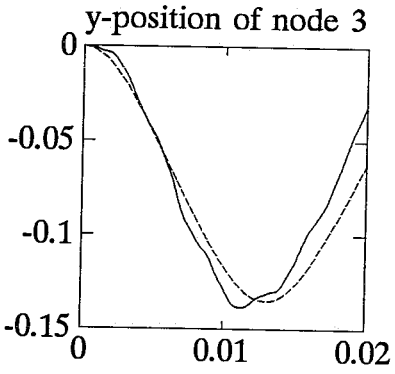


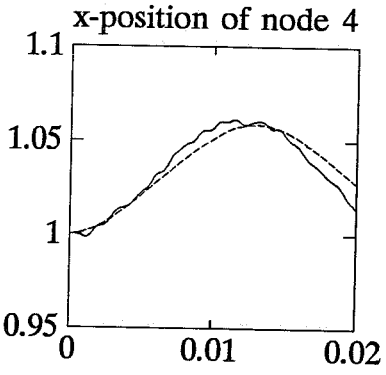


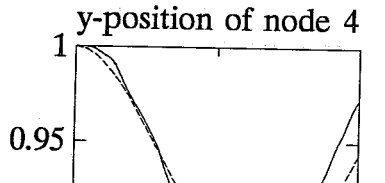


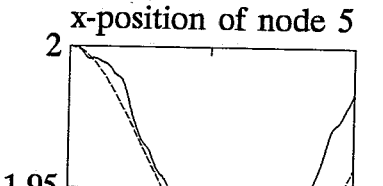


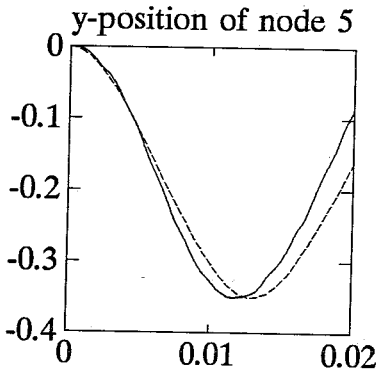


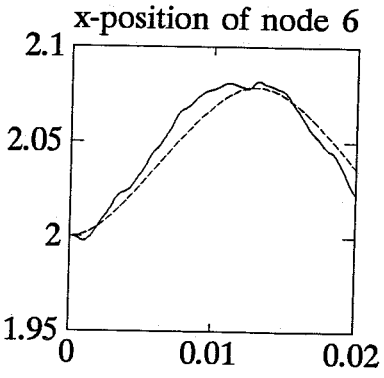


Fig. B.6 — *direct integration of original system*
*- - direct integration of reduced system*

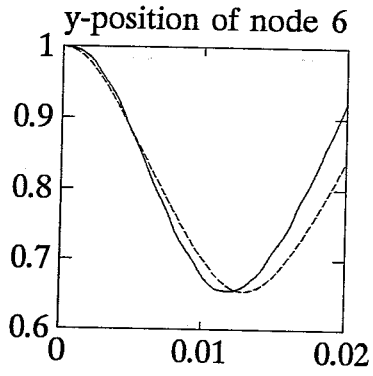


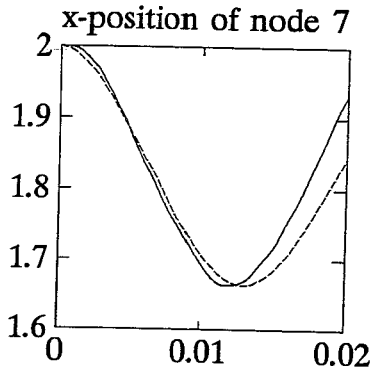


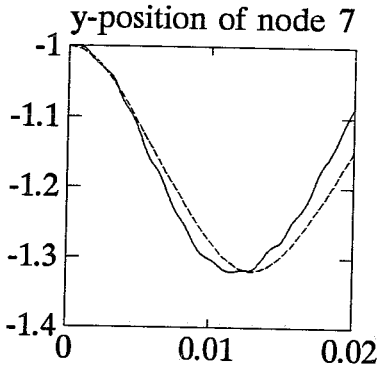


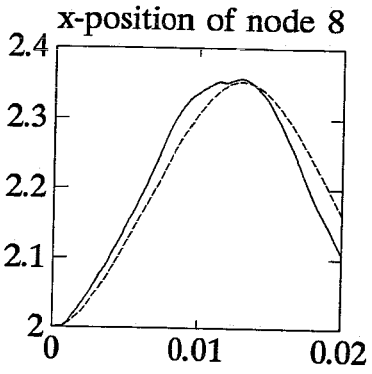


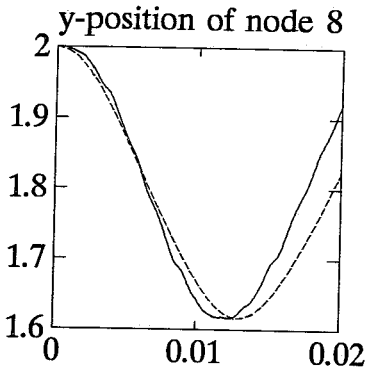


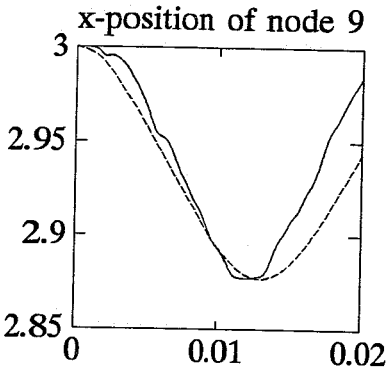


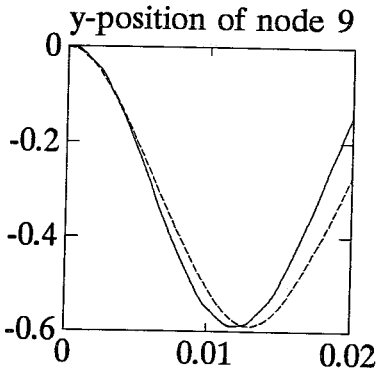


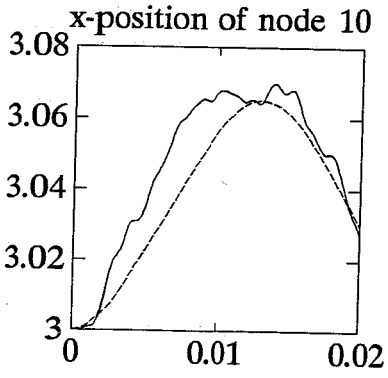


Fig. B.7 — *direct integration of original system*
*- - direct integration of reduced system*

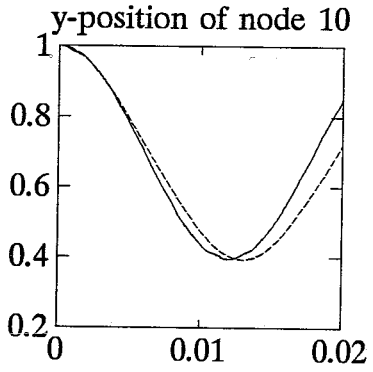


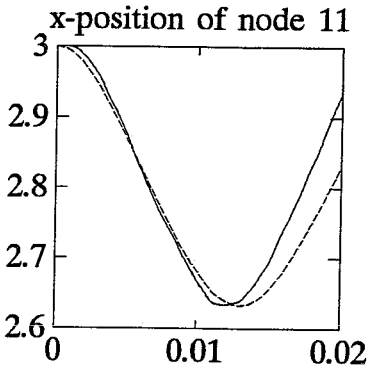


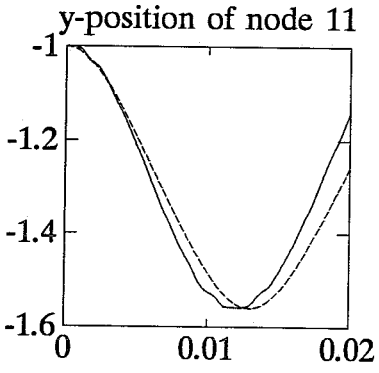


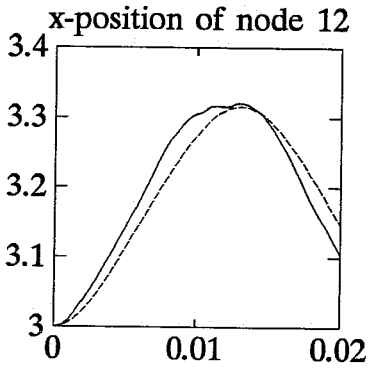


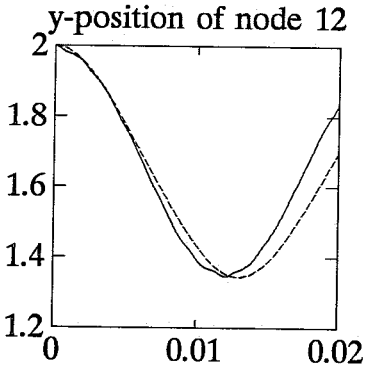


Fig. B.8 — *direct integration of original system*
*- - direct integration of reduced system*

## B.3 Simulation 3

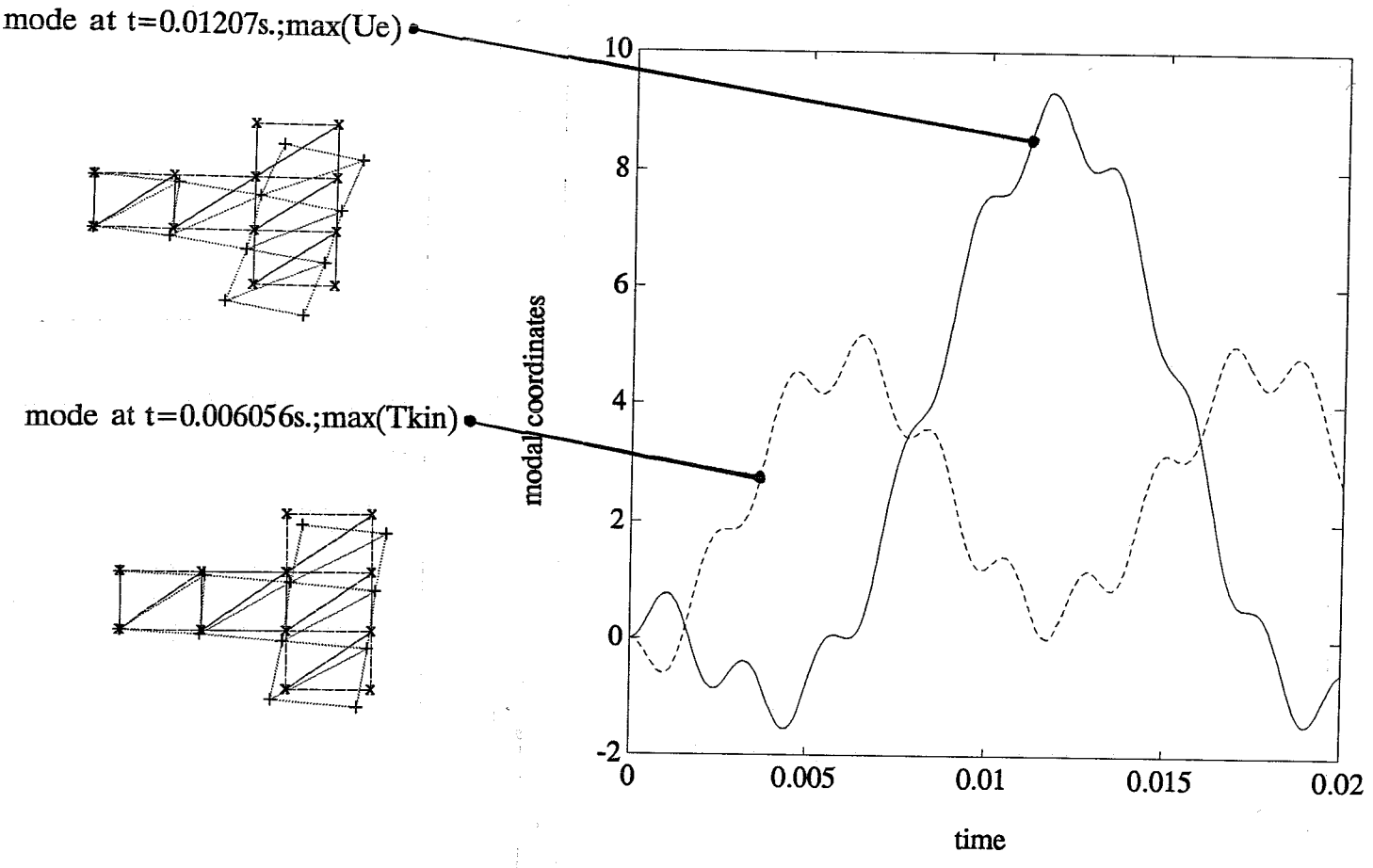


Fig. B.9 *modes and modal coordinates*

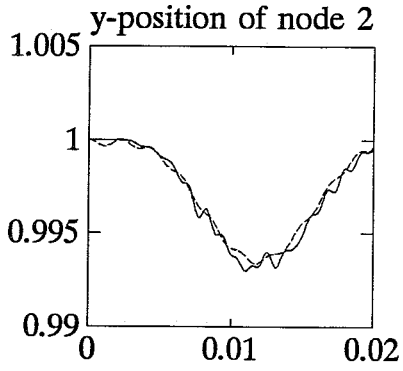


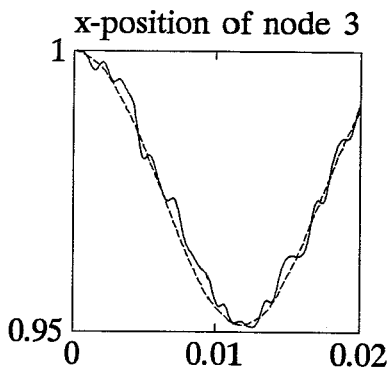


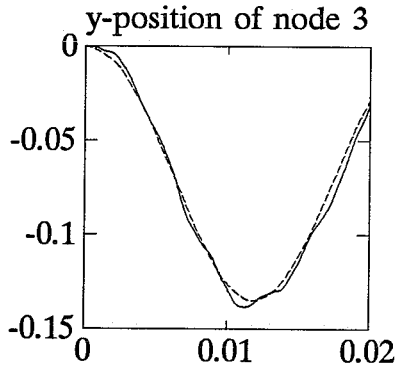


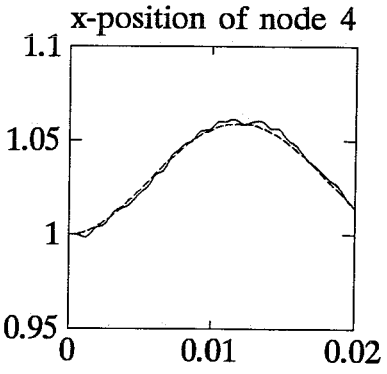


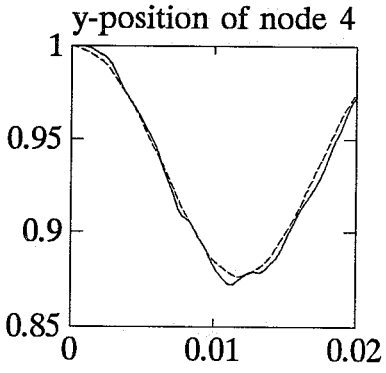


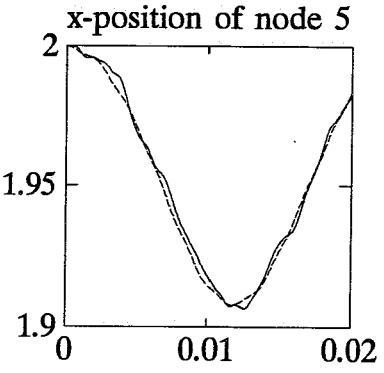


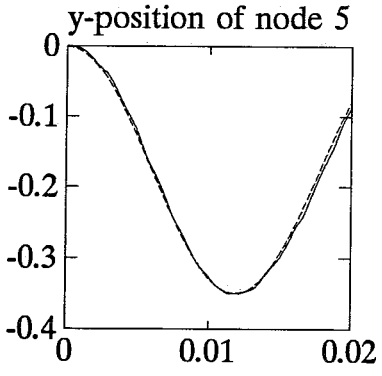


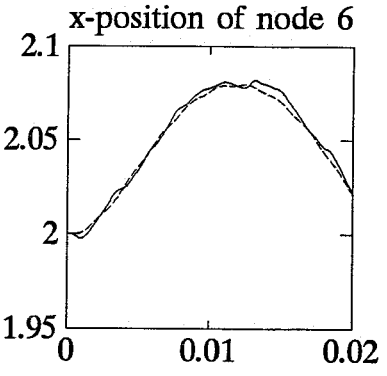


Fig. B.10 — *direct integration of original system*
*- - direct integration of reduced system*

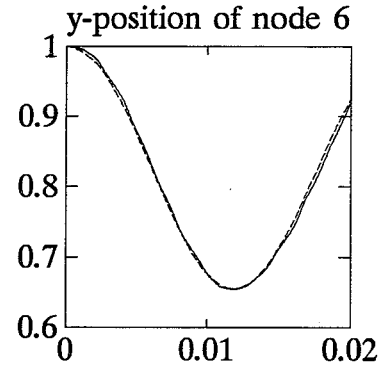


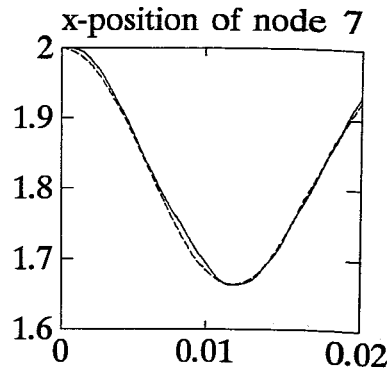


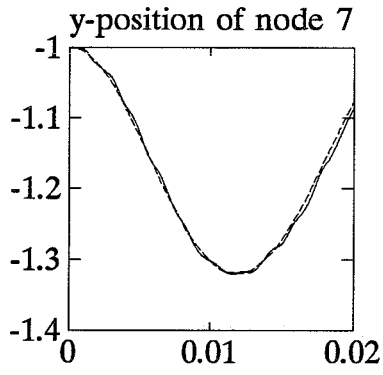


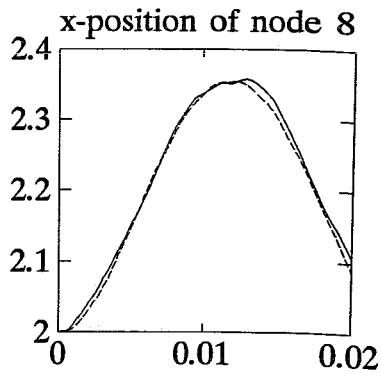


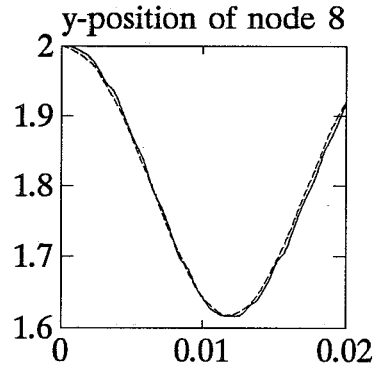


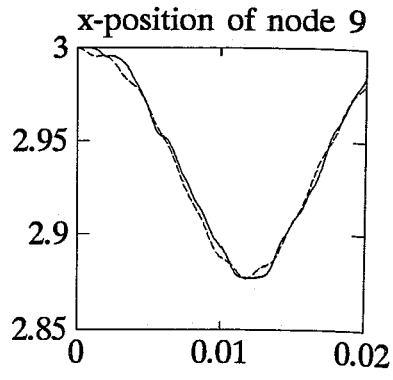


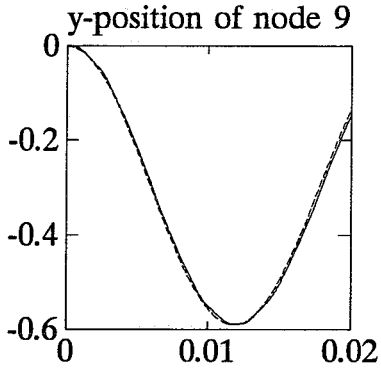


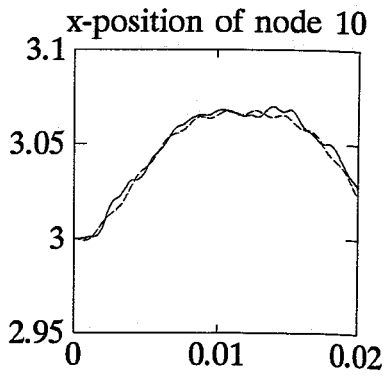


Fig. B.11 — *direct integration of original system*
- - *direct integration of reduced system*

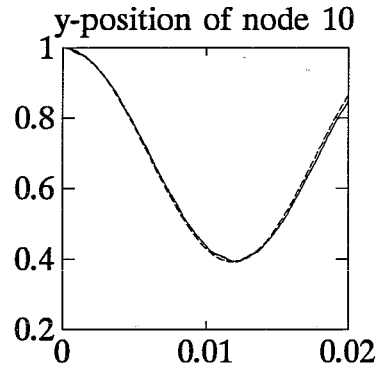


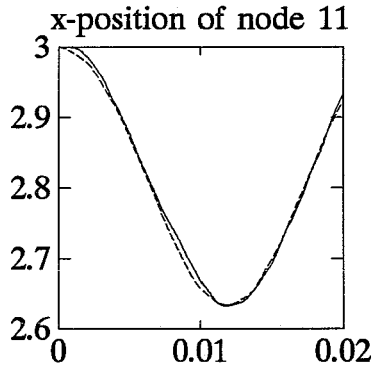


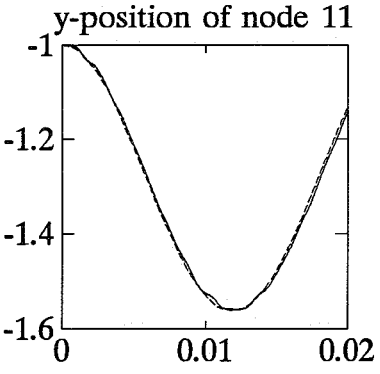


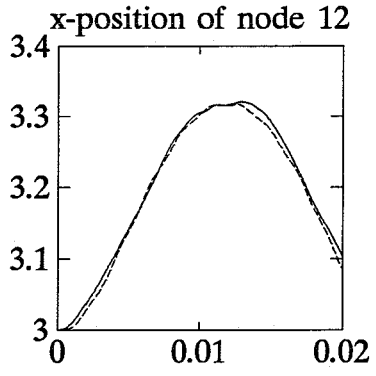


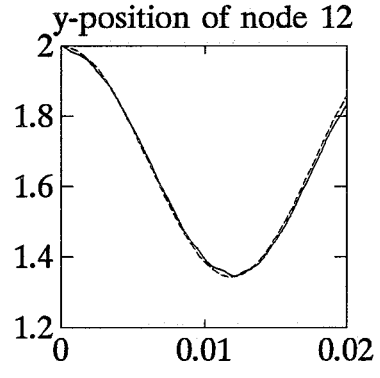


Fig. B.12 — *direct integration of original system*
*- - direct integration of reduced system*

## B.4 Simulation 4

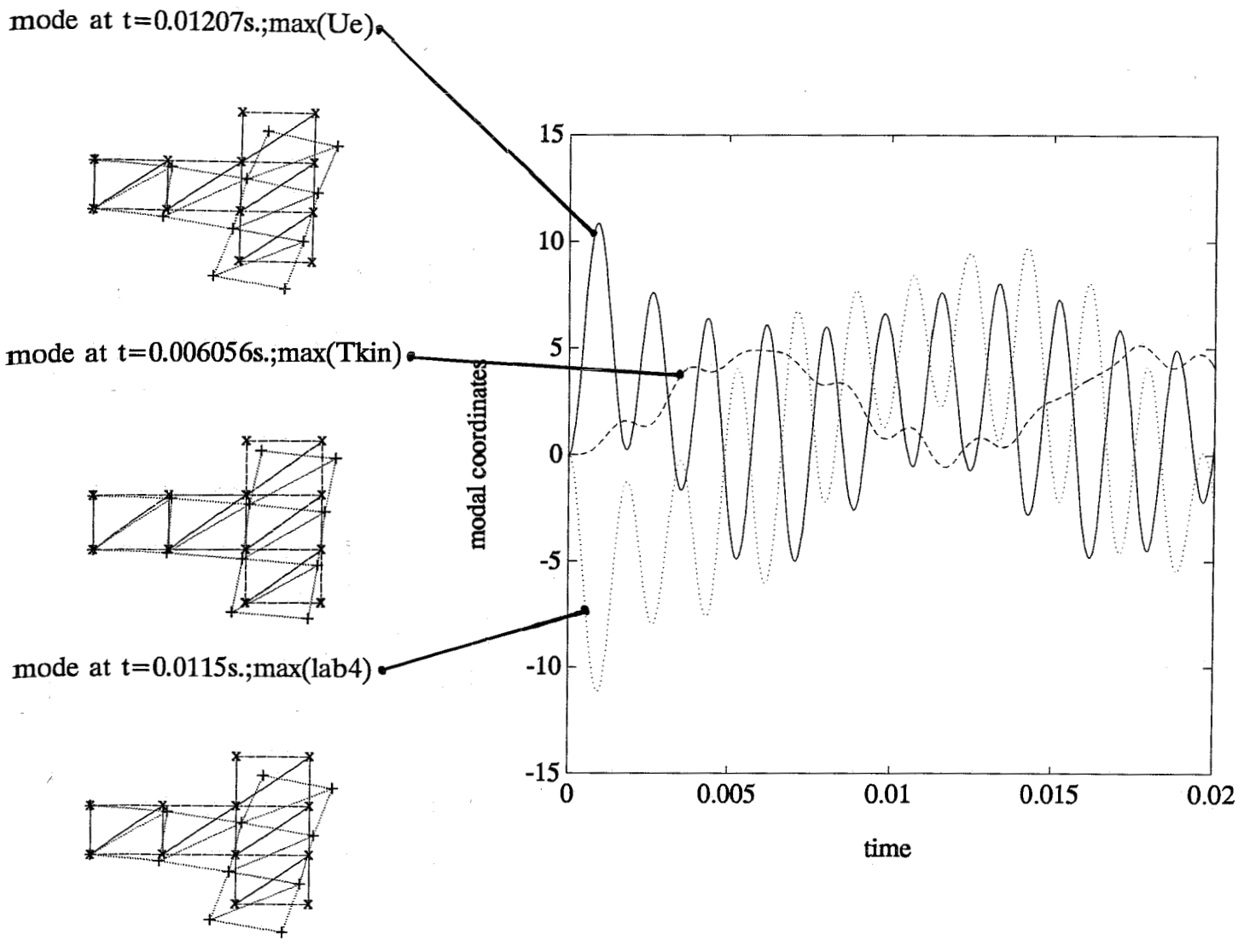


Fig. B.13 *modes and modal coordinates*

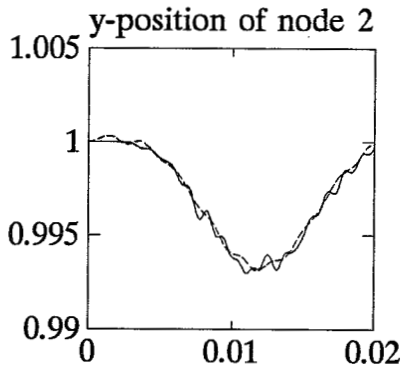


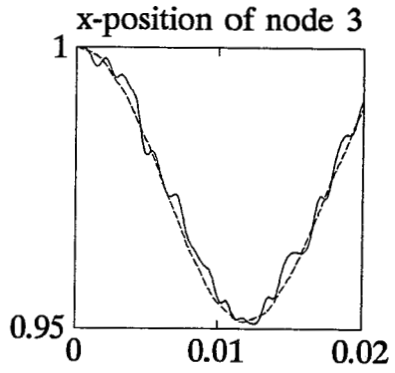


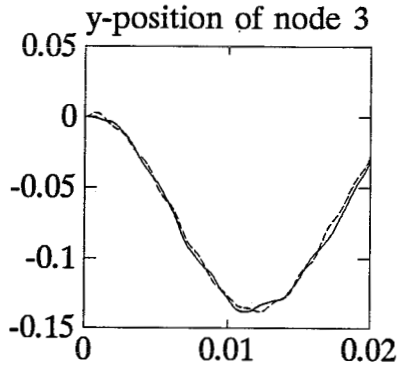


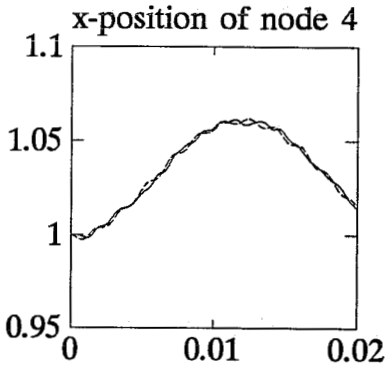


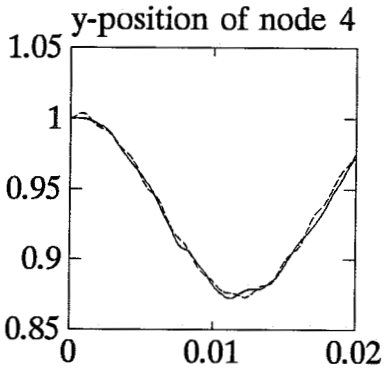


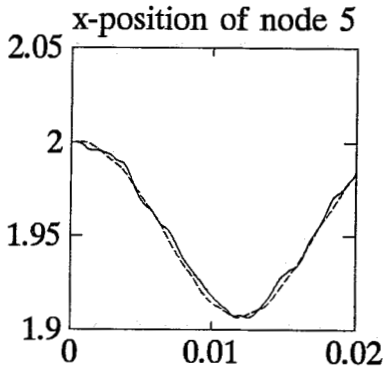


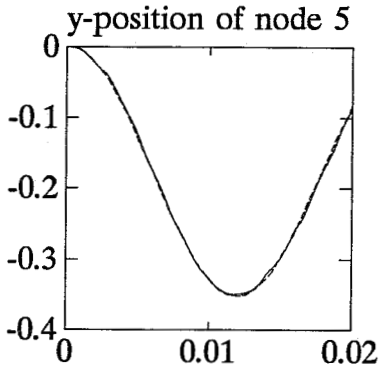


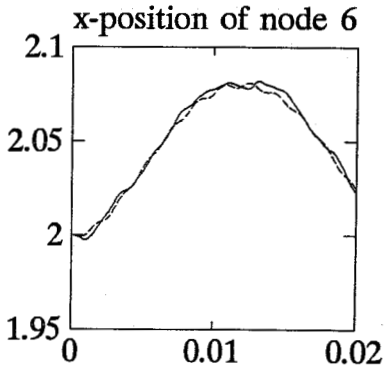


Fig. B.14 — *direct integration of original system*
*- - direct integration of reduced system*

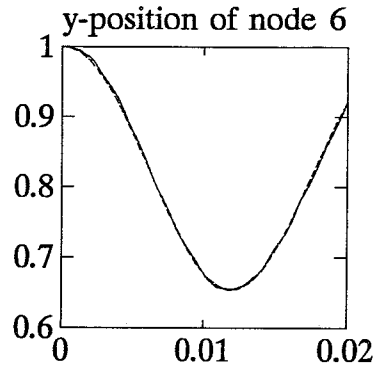


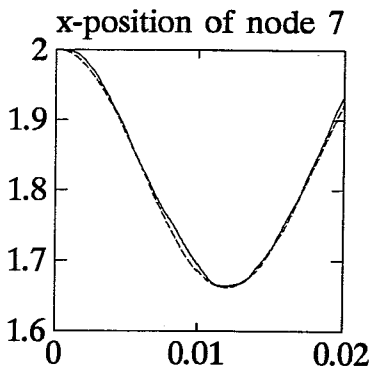


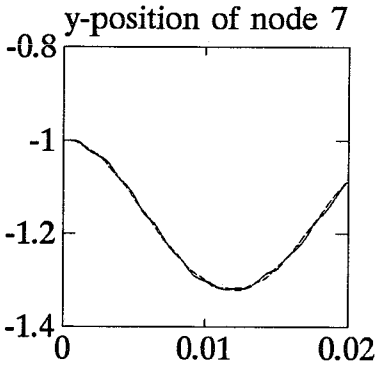


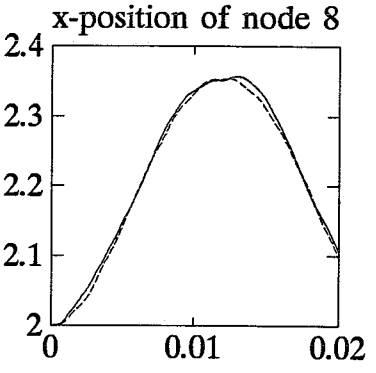


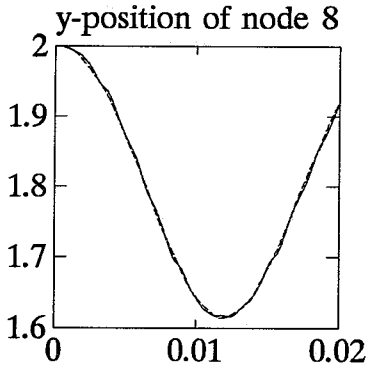


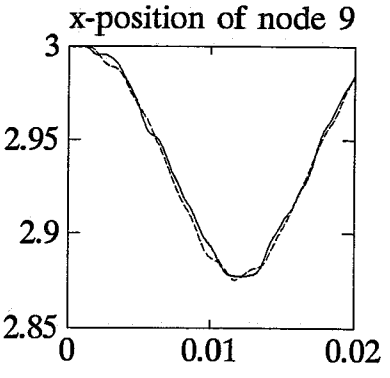


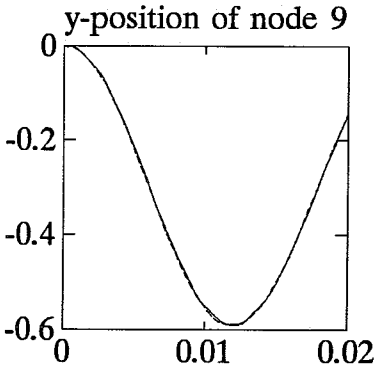


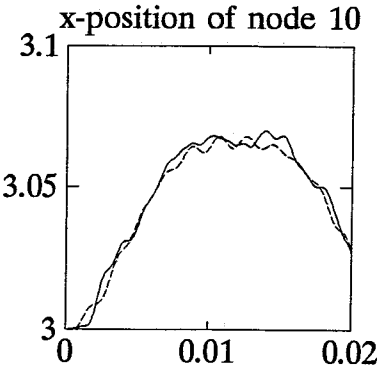


Fig. B.15 — *direct integration of original system*
- - *direct integration of reduced system*

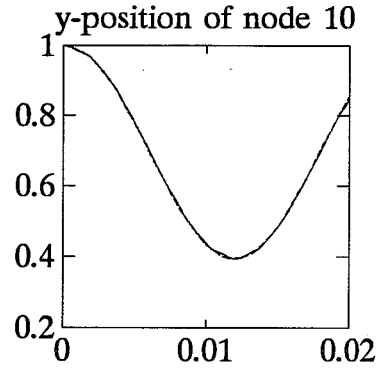


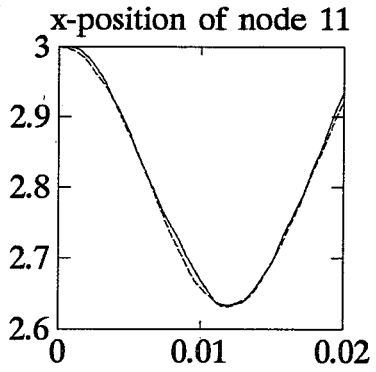


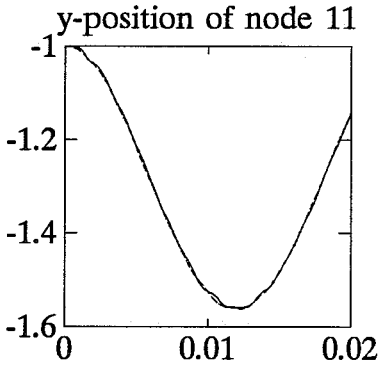


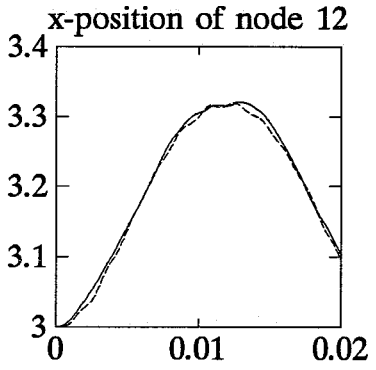


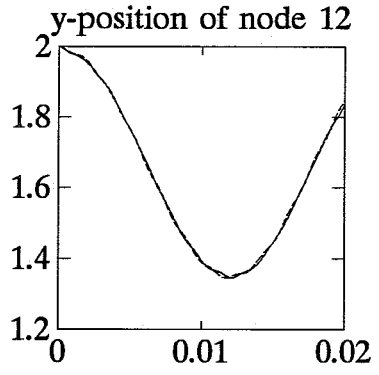


Fig. B.16 — *direct integration of original system*
*- - direct integration of reduced system*